EFFECTS OF CHOLINE KINASE ACTIVITY ON PHOSPHOLIPID METABOLISM AND MALIGNANT PHENOTYPE OF PROSTATE CANCER CELLS

Aditya Bansal

Submitted to the faculty of the University Graduate School
in partial fulfillment of the requirements
for the degree
Doctor of Philosophy
in the Department of Biochemistry and Molecular Biology,
Indiana University

October 2010

Accepted by the Faculty of Indiana University, in partial
fulfillment of the requirements for the degree of Doctor of Philosophy.

Timothy R. DeGrado, Ph.D., Chair
Department of Biochemistry and Molecular Biology

Robert A. Harris, Ph.D.
Department of Biochemistry and Molecular Biology

Doctoral Committee

William F. Bosron, Ph.D.
Department of Biochemistry and Molecular Biology

June 15, 2010

James E. Klaunig, Ph.D.
Department of Toxicology

DEDICATION

This study is dedicated to my family and friends for their unconditional love and support; to my wife Pragya Sharma for her love, encouragement, and patience; to my child, Sabhya Bansal, for bringing joy to my life; to my sister Megha Bansal for her love, support and encouragement.

ACKNOWLEDGEMENTS

I am indebted to many people who have helped me throughout my graduate study. My sincere appreciation goes to all of them.

- Dr. Timothy R. DeGrado for his wonderful mentoring, enormous support, and being my role model.
- Dr. Robert A. Harris for his great discussion, helpful criticism and suggestions.
- Dr. William F. Bosron and Dr. James E. Klaunig for their valuable advices and reference.
- All current and previous members in laboratory of Dr. Timothy R. DeGrado
- All members in laboratory of Dr. Robert A. Harris.
- All members in laboratory of Dr. William F. Bosron.

ABSTRACT

Aditya Bansal

EFFECTS OF CHOLINE KINASE ACTIVITY ON PHOSPHOLIPID METABOLISM AND MALIGNANT PHENOTYPE OF PROSTATE CANCER CELLS

High choline uptake and increased choline kinase activity have been reported in many cancers. This has motivated the use of choline as a biomarker for tumor imaging. Tumors in general are heterogeneous in nature with respect to oxygen tension. There are regions of hypoxia and normoxia that are expected to have different metabolism but regulation of choline metabolism under hypoxia is poorly understood. It is important to clarify the status of choline metabolism in hypoxic microenvironment as it will have an impact on potential of choline as a cancer biomarker. The primary goal was to determine the status of choline phosphorylation in hypoxic cancer cells and its effect on uptake of choline. This was examined by tracer studies in cancer cells exposed to hypoxia. It was observed that hypoxia universally inhibits choline uptake /phosphorylation in cancer cells. Decreased choline phosphorylation resulted in transient uptake of choline radiotracers in cultured cancer cells and 9L tumors suggesting potential problem in using choline as a biomarker for cancers in hypoxic microenvironment. To investigate the mechanism behind decrease in choline phosphorylation, steady state levels of choline metabolites were measured and choline kinase catalyzed choline phosphorylation step was found to be rate-

limiting in PC-3 cells. This suggested that modulation in choline kinase levels can alter choline metabolism in hypoxic cancer cells. Expression and activity assays for choline kinase revealed that choline kinase expression is down-regulated in hypoxia. This regulation involved transcriptional level mediation by HIF1 at the conserved HRE7 site in choline kinase promoter. To further understand the importance of down-regulation of choline kinase in hypoxia, stable prostate cancer cell lines over-expressing choline kinase were generated. Effect of over-expression of choline kinase in hypoxia was evaluated in terms of malignant phenotypes like proliferation rate, anchorage independent growth and invasion potential. Both over-expression of choline kinase and hypoxia had a pronounced effect on malignant phenotypes of prostate cancer cells. Further study showed that increased choline kinase activity and hypoxic tumor microenvironment are important for progression of early-stage, androgen-dependent LNCaP prostate cancer cells but confer little survival advantage in undifferentiated, androgen-independent PC-3 prostate cancer cells.

Timothy R. DeGrado, Ph.D., Chair

TABLE OF CONTENTS

LIST OF TABLES

LIST OF FIGURES

GENERAL INTRODUCTION

1. Phosphatidylcholine metabolism

1.1. Overview of phosphatidylcholine metabolism

Phosphatidylcholine is quantitatively the most important membrane lipid in eukaryotic cells (Pelech and Vance, 1984). The majority (40-60%) of the eukaryotic membrane phospholipids are phosphatidylcholines (Kent, 2005). The biosynthesis of phosphatidylcholine in eukaryotes is done by two distinct pathways - CDP-choline pathway (also known as Kennedy pathway) (Figure 1A) and successive methylation of phosphatidylethanolamine to phosphatidylcholine (Figure 1B). Among the two, the CDP-choline pathways represents the major phosphatidylcholine synthesis pathway in eukaryotes (Kent, 2005).

1.2. Reactions of CDP-choline pathway

The CDP-choline pathway consists of three steps: 1. phosphorylation of choline to form phosphocholine, catalyzed by choline kinase; 2. transfer of CMP from CTP to phosphocholine to form CDP-choline, catalyzed by CTP-phosphocholine cytidylyltransferase (CCT); and 3. transfer of phosphocholine from CDP-choline to diacylglycerol to form phosphatidylcholine , catalyzed by CDP-choline: *sn*-1,2-diacylglycerol choline phospho-transferase (Figure 1A) (Kent, 2005).

A CDP Choline pathway
(Kennedy pathway)

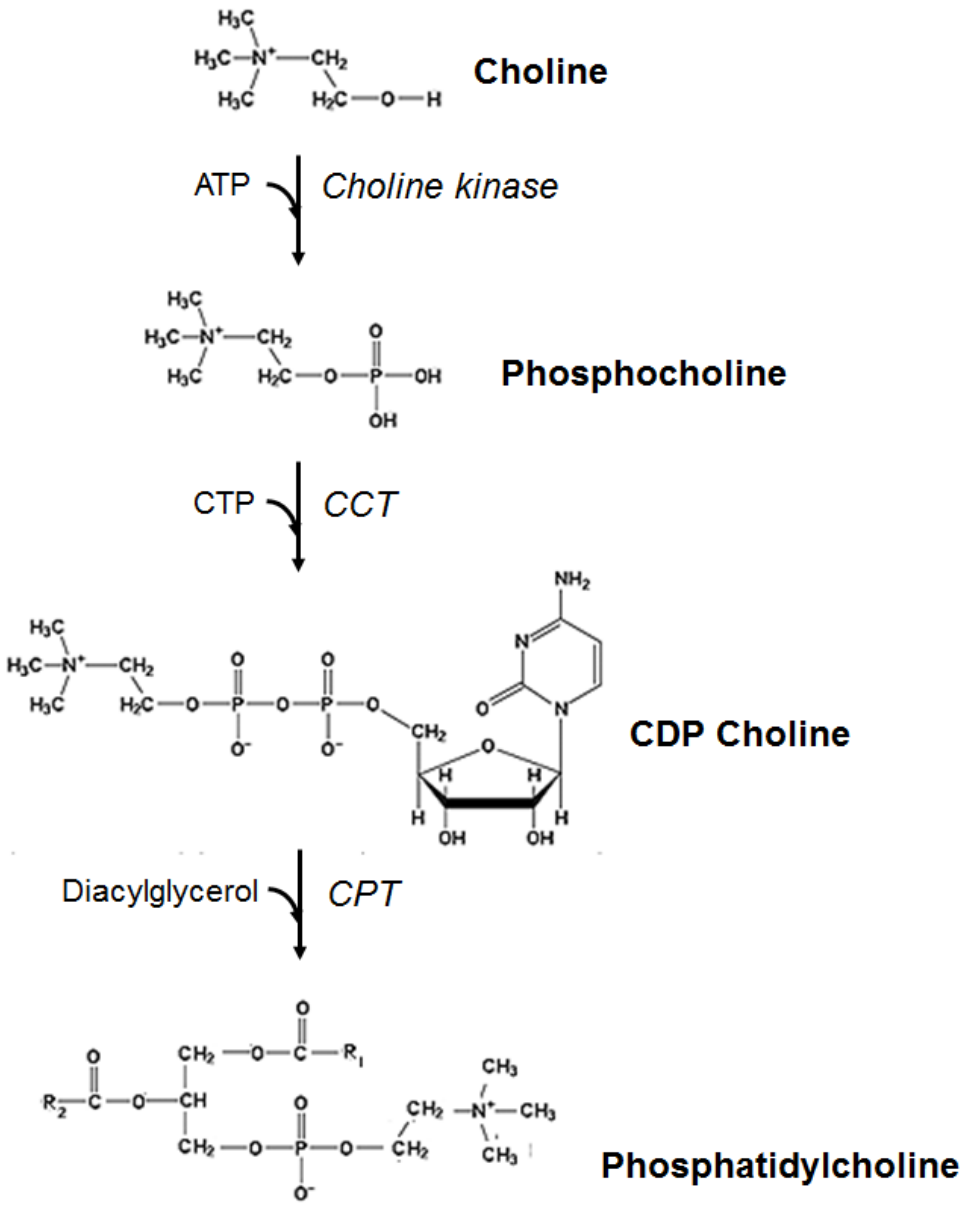

B Methylation of Phosphatidylethanolamine (PtdEtn)

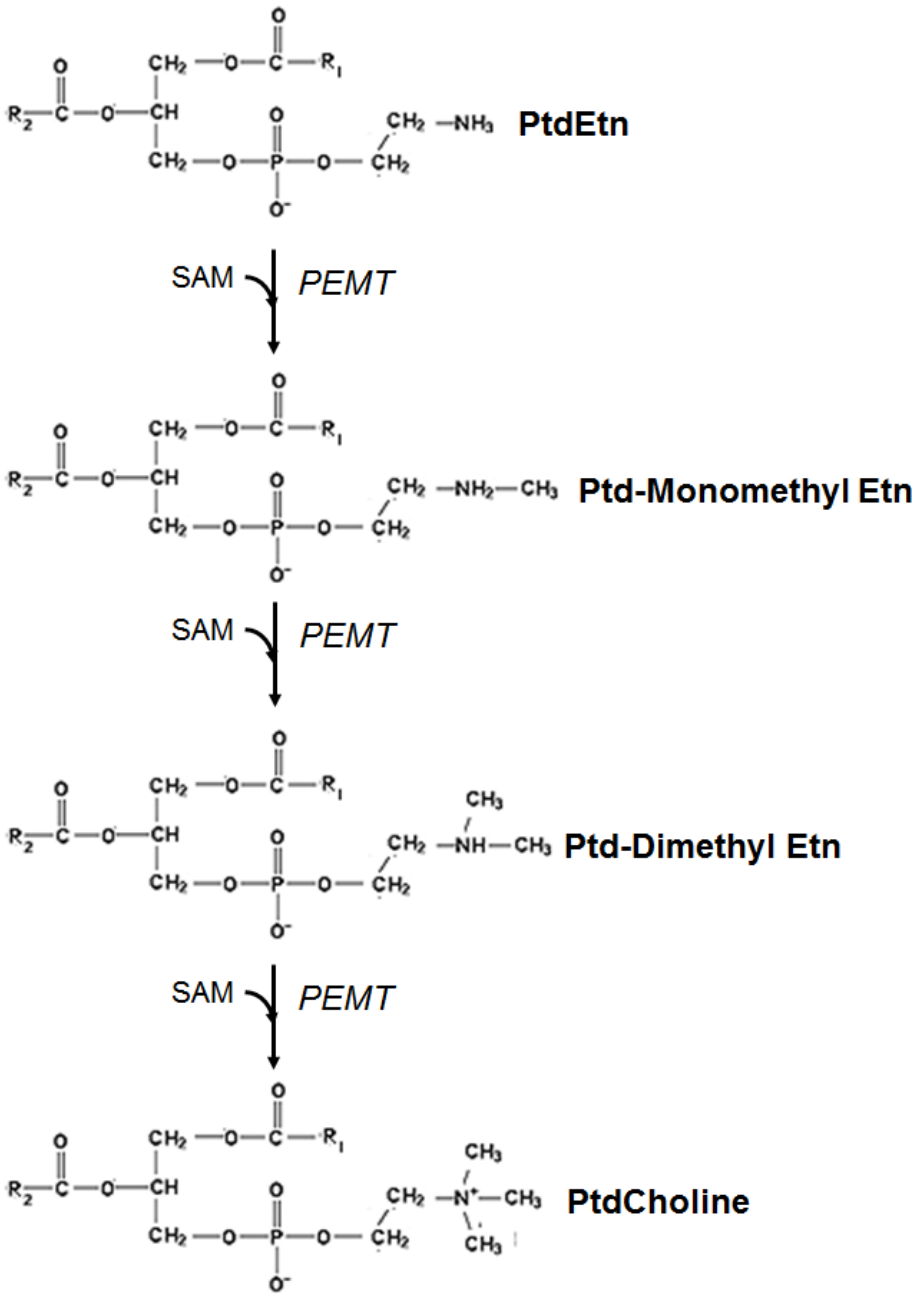

Figure 1. Biosynthesis of phosphatidylcholine in eukaryotes. (A) CDP-choline pathway and (B) successive methylation of phosphatidylethanolamine. ATP = Adenosine triphosphate, CTP = Cytosine triphosphate, CCT = CTP-phosphocholine cytidylyltransferase, CPT = CDP-choline: *sn*-1,2-diacylglycerol choline phospho- transferase, SAM = S-Adenosyl Methionine, PEMT - Phosphatidylethanolamine Methyltransferase. Modified from Kent, 2005.

1.3. Regulation of CDP-choline pathway

1.3.1. Regulatory reactions in CDP-choline pathway

The two regulatory enzymes in the CDP-choline pathway are choline kinase and CCT. Traditionally, CCT was believed to be the rate-limiting enzyme in phosphatidylcholine biosynthesis with choline kinase having low control strength in the flux in CDP-choline pathway (Ishidate, 1997). Presence of inactive cytosolic and active membrane bound form of CCT (Wilgram and Kennedy, 1963), and activation of CCT by certain phospholipids (Fiscus and Schneider, 1966) established CCT as an important regulatory enzyme for phosphatidylcholine synthesis. Later evidence grew to support choline kinase as also being rate-limiting (Infante, 1977; Infante and Kinsella, 1978) and regulatory in some circumstances for instance in phosphatidylcholine synthesis in mitogen stimulated NIH3T3 cells (Warden and Friedkin, 1985) and *ras* oncogene expressing mouse fibroblasts (Ratnam and Kent, 1995).

1.4. Choline kinase (ChK)

1.4.1. Overview of choline kinase

Located in the cytoplasm, choline kinase catalyzes phosphorylation of choline in the presence of ATP and Mg^{2+} (Wittenberg and Kornberg, 1953). Mammalian choline kinase has 3 isoforms: ChK isoforms α1 (ChKα1); ChK isoforms α2 (ChKα2); and ChK isoformβ (ChKβ). ChKα1 and ChKα2 are splice variants with addition of 18-residue segment (RSCNKEGSEQAQNENEFQ) in the amino-half of the ChK α2 protein. ChK α1 is shorter than ChK α2 and is 60%

homology to ChKβ (Aoyama et al., 1998). The 2.7-kb gene encoding human ChK α is located on chromosome 11 and has 12 exons (NCBI). The 1.6-kb gene encoding human ChKβ is located on chromosome 22 and has 11 exons (NCBI). Choline kinase exists in homo- or hetero-dimeric forms (Aoyama et al., 2002). The proportion of the different homo- (αα or ββ) or hetero- (αβ) dimer population has been proposed to be tissue-specific (Aoyama et al., 2002). Furthermore, the combination between choline kinase isoforms results in a different level of choline kinase activity *in vitro* under cell-free systems conditions. The α/α homodimer is the most active choline kinase form, the β/β homodimer the less active, and the α/β heterodimer has an intermediate phenotype (Aoyama et al., 2002). Distribution of isoform's dimer population is still not known but ChKα is the major form of choline kinase which positively correlates with malignant phenotype of cancer cells (Figure 2).

1.4.1.2. Structure of choline kinase

Choline kinase has an N-terminal domain and a C-terminal domain, with an active site situated between the two domains (Figure 3) (Peisach et al., 2003). The N-terminal domain is composed of a five-stranded antiparallel β-sheet (β-strands A-E) and a single α-helix (helix 1). Inserted between the third (C) and the fourth (D) strands of this β-sheet is an α-helix that forms the interface stabilizing the protein as a dimer (helix 2). Amino acids belonging to the region connecting the third β-strand with the interface helix are not visible in electron density maps of all three structures. Interestingly, this sequence segment represents the 18 amino acids missing in α1. This insertion in hChKα2 lowers the K_m for choline to

0.10 mM, in comparison to the much higher value of 1.69 mM for hChKα1. The C-terminal domain is primarily helical, and contains many of the conserved and functionally important residues. The loop comprising residues 302-311 is the Brenner's motif, whereas the region including residues 326-354 is the choline kinase motif. Recently the apo structure of the nematode *C. elegans* choline kinase (CKA2), which exhibits 42% sequence identity with hChKα2, has been reported (Malito et al., 2006).

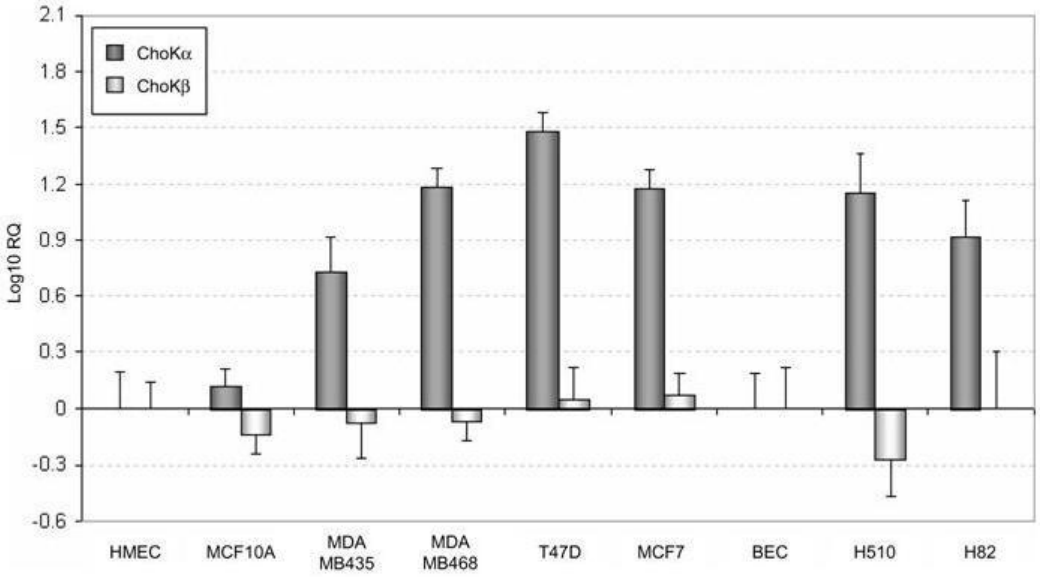

Figure 2. Expression profile of choline kinase isoforms mRNA in various breast cancer cell lines. Choline kinase α isoform is upregulated in majority of breast cancer cell lines. Modified from Gallego-Ortega et al., 2009. The data in Y-axis were normalized with the endogenous 18S ribosomal RNA. For the comparison between tumoral and non-tumoral cell line (HMEC), the $2^{-\Delta\Delta Ct}$ method was applied and log10 RQ (relative quantity) represents Log_{10} of (mRNA signal in tumoral cells/mRNA signal in HMEC). ChKα represents both choline kinase alpha1 and alpha2 while ChKβ represents choline kinase beta isoform.

Comparison of the isoforms of choline kinase showed 5 conserved motifs, ATP-binding loop, dimer interface, link, Brenner's motif and choline kinase motif (Figure 4). Out of these , Brenner's phosphotransferase motif and putative choline kinase motif are reported to be part of catalytic domains (Aoyama et al., 2004). The functions of other conserved motifs are currently unknown. Recently, X-ray diffraction analysis of crystallized isoform of *Caenorhabditis elegans* choline kinase (CKA2) has shown involvement of these domains in the formation of active dimer complex (Peisach et al., 2003).

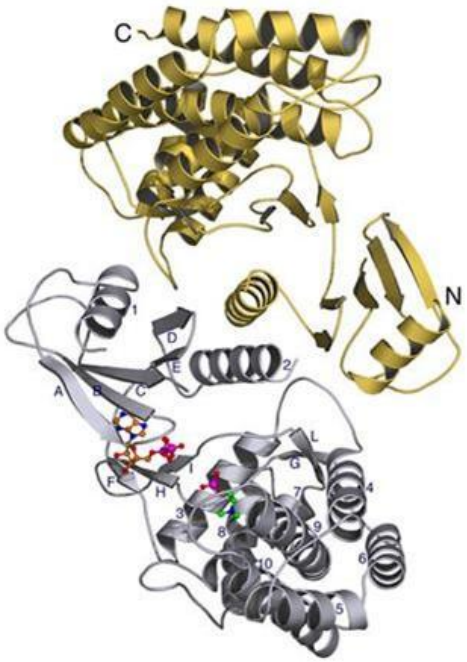

Figure 3. A stereo ribbon drawing of human choline kinase α dimer. α helices are numbered and drawn as coils, β strands are lettered and drawn as arrows, and other elements are drawn as tubes. ball-and-stick representation of ADP and PCho molecules are shown with their carbon atoms colored in orange and green, respectively. Oxygen, nitrogen and phosphate atoms are shown in red, blue and magenta, respectively. Modified from Malito et al., 2006.

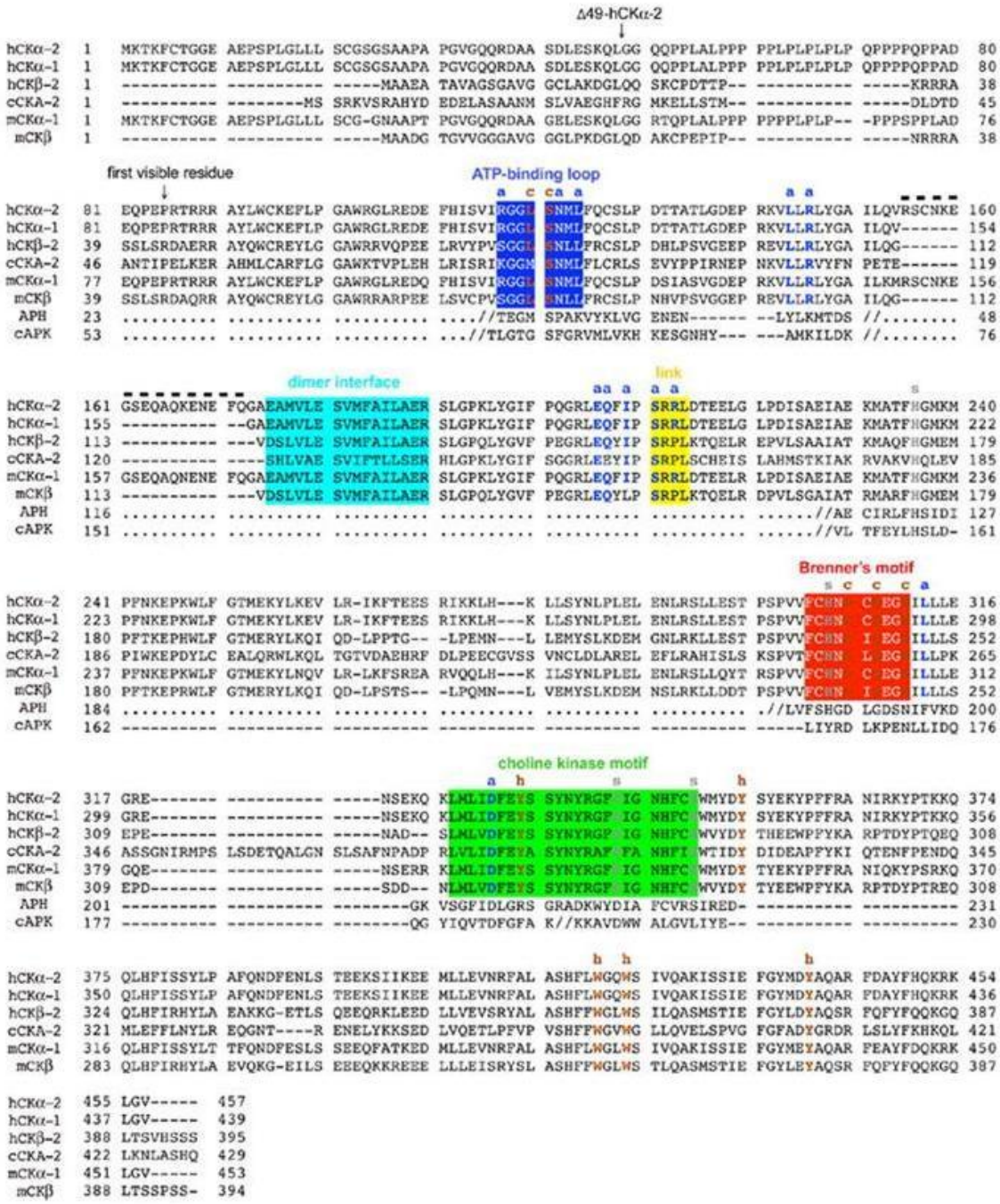

Figure 4. Amino acid alignment of choline kinase isoforms. Alignment of human choline kinase isoforms (hCKα2, α1, β2), C. elegans choline kinase isoform alpha-2 (cCKA2), mouse choline kinase isoform alpha-1 and beta (mCKα1 and mCKβ), atypical enzymes - aminoglycoside 3'phospho transferase (APH) and cAMP-dependent protein kinase (cAPK) showing conserved ATP-binding loop, dimer interface, link, Brenner's motif and choline kinase motif. The alignment shows that atypical enzyme that show resemblance in structure do not share any sequence homology. Modified from Malito et al., 2006.

Choline kinase is known to be an enzyme primarily responsible for catalyzing phosphorylation of choline. No other substrate of choline kinase is known. Although protein phosphorylation ability of choline kinase has not yet confirmed but based on structure of choline it is possible that it can potentially phosphorylate proteins too. This is because structure of choline kinase reveals a typical protein kinase fold found in “atypical kinases” (AKs) family of enzymes (Malito et al., 2006) (Figure 5). These “atypical kinases” clearly share homology with the eukaryotic protein kinases (ePKs) catalytic core but do not conserve all of the usual kinase motifs (Figure 5).

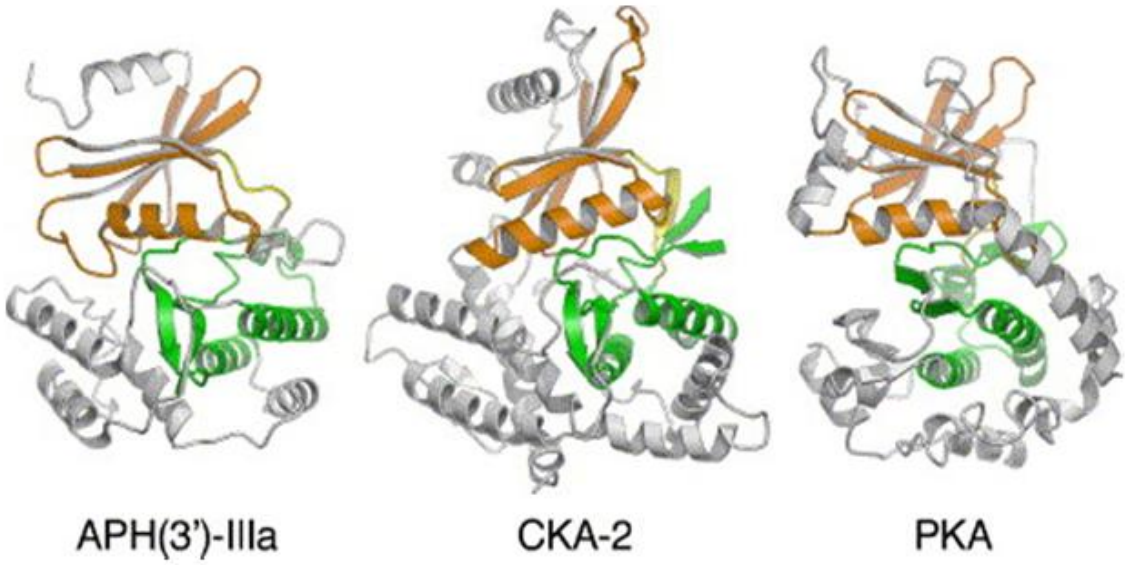

Figure 5. Comparison of structure of choline kinase, aminoglycoside 3’phospho transferase (APH(3’)-IIIa) and the catalytic domain of cAMP-dependent protein kinase (PKA). Modified from Kent, 2005.

1.4.1.3. Mechanism of reaction catalyzed by choline kinase

Kinetic mechanism of choline kinase from rat striata (Reinhardt et al., 1984) was studied under steady state conditions using various concentrations of ATP- Mg^{2+} at several concentrations of free Mg^{2+} and a single concentration of choline (Reinhardt et al., 1984). The initial velocity, product, and dead-inhibitor studies with choline kinase suggested that the forward reaction follows an initial random ordered mechanism followed by sequential ordered mechanism (Figure 6). ATP- Mg^{2+} and choline binding to the enzyme first in random order, followed by sequential order of activation of the ternary complex by free Mg^{2+}. The release of phosphocholine occurred prior to that of ADP- Mg^{2+}. Thus, the overall rate of reaction was probably limited by the release of ADP- Mg^{2+} from the complex (Ishidate and Nakazawa, 1992).

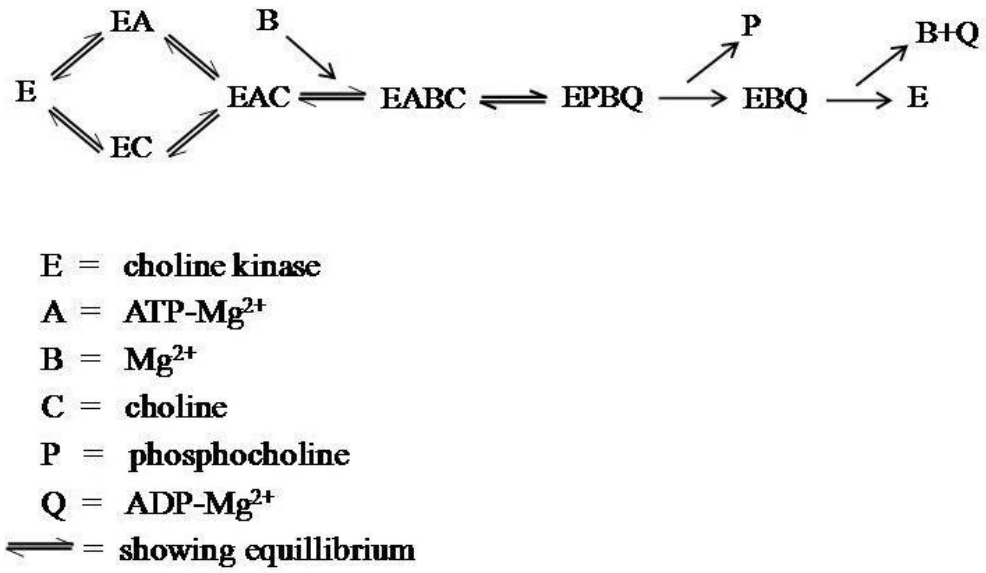

Figure 6. Schematic diagram showing the reaction mechanism of choline kinase. Modified from Ishidate and Nakazawa, 1992.

1.4.1.4. Kinetic parameters of choline kinase

Highly purified choline kinase preparations from different mammalian tissue sources have multiple Km's (Table 1). The multiple Km's could be explained either by the presence of two catalytic species (or sites) with different affinities for choline and ATP (Ishidate and Nakazawa, 1992; Ishidate et al., 1985 ; Tadokoro et al., 1985) or by a mechanism of negative cooperativity between choline binding sites (Ishidate and Nakazawa, 1992 ; Ishidate et al., 1985). Homogenous preparation of choline kinase from rat kidney has been shown to have two binding sites for choline, probably one catalytic and other regulatory (Ishidate et al., 1985). Choline kinase has highest activity at alkaline pH (8.0-9.5) as seen in *in vitro* assays and the activity is considerably reduced at neutral pH. The highest activity is obtained with an ATP/ Mg^{2+} ratio of 1.0 and excess ATP is inhibitory. Out of the two isoforms, ChKα has the ability to phosphorylate both choline and ethanolamine but ChKβ prefers ethanolamine for phosphorylation (Table 2). Ethanolamine is also phosphorylated by ethanolamine kinase, and phosphoethanolamine follows the CDP-ethanolamine pathway to form phosphatidylethanolamine.

Table 1. Kinetic parameters of choline kinase reaction obtained with highly purified or recombinant enzyme preparations. Modified from Aoyama et al., 2004.

Source of ChK	Specific activity (mmol/min/mg)	Equilibrium constant (Km)	
		Choline(μM)	ATP (mM)
Rat kidney	3.3	100	1.5
Rat liver	143	13	0.048
Rat brain	40	14	1
S. cerevisiae	128	270	0.09
C. elegans	43	1.6 mM	2.4

Table 2. Kinetic characteristic of choline kinase isoforms, ChKα and ChKβ Modified from D Gallego-Ortega et al., 2009

Substrate	Isoform	Equilibrium constant (Km)	Standard error
Choline	ChKα	0.20	0.04
	ChKβ	0.57	0.08
Ethanolamine	ChKα	12.01	2.14
	ChKβ	2.01	0.42

1.4.1.5. Choline kinase knockouts

ChKα and ChKβ are expressed in a tissue specific manner. Recently, knockout studies in mice contributed to understanding of the individual role of isoform towards phosphatidylcholine synthesis and viability. ChKβ knockout (KO) mice (*rmd* mice) are viable, but develop a rostrocaudal muscular dystrophy, while

phosphatidylcholine levels are normal in most tissues analyzed except in hind limb skeletal muscle (Malito et al., 2006). Therefore, ChKα is sufficient to maintain normal phosphatidylcholine levels in most tissues. By contrast, the lack of ChKα results in embryonic lethality, and ChKα$^{+/-}$ heterozygous mice displays an accumulation of choline and a reduction in phosphocholine in liver and testis, suggesting that there is no ChKβ compensation in ChKα knockouts for phosphatidylcholine biosynthesis *in vivo*. These results suggest different roles *in vivo* for both ChKα and ChKβ isoforms. Furthermore, the attenuated levels in phosphatidylethanolmine found in ChKα$^{+/-}$ heterozygous mice suggest the involvement of ChKα not only in the biosynthesis of phosphatidylcholine but also in the phosphatidylethanolmine pathway (Malito et al., 2006). This is also consistent with the fact that in ChKβ KO mice, phosphatidylethanolmine levels are unaffected, indicating that phosphatidylethanolmine homeostasis is fully maintained with the ethanolamine kinase and ChKα proteins intact.

1.4.2. Regulation of choline kinases

1.4.2.1. Regulation of choline kinase activity by allosteric effectors

Yeast choline kinase is known to be allosterically regulated by ATP and ADP molecules in a positive cooperative manner. The positive cooperative kinetics exhibited by the purified choline kinase with respect to ATP is a property common to many nucleotide-dependent allosteric enzymes (Traut, 1994; Kim et al., 1998). Cooperative kinetics is generally attributed to the association of enzyme subunits to form oligomeric structures (Traut, 1994; Kim et al., 1998). Indeed, the relative amounts of the tetrameric and octomeric forms of the purified

yeast choline kinase increased in the presence of ATP. With respect to regulation by ADP, the purified choline kinase was inhibited by ADP, the product of the reaction. The regulation of choline kinase activity by ATP and ADP may be physiologically relevant. Extrapolating this to mammalian choline kinase, high Km for ATP and allosteric regulation by ATP and ADP allows choline kinase to respond to changes in energy status.

1.4.2.2. Regulation of choline kinase activity by phosphorylation

Phosphorylation is a major mechanism by which enzymes are regulated (Choi et al., 2005). Choline kinase from *S. cerevisiae* (yeast) is known to be regulated by phosphorylation (Choi et al., 2005). Choline kinase is phosphorylated on multiple serine residues *in vivo*, and some of this phosphorylation is mediated by protein kinase A. Protein kinase A phosphorylates and stimulates (~2-fold) choline kinase at Ser^{30} and Ser^{85}, with the former site having the major effect on enzyme regulation. Moreover, phosphorylation at these sites stimulates phosphatidylcholine synthesis via the Kennedy pathway. Recently, phosphorylation of yeast choline kinase at Ser^{30} was shown to be also mediated by protein kinase C along with Ser^{25} (Choi et al., 2005). In addition, S25A mutation in choline kinase decreased phosphatidylcholine synthesis by the Kennedy pathway due to inhibition of choline kinase activity. Protein kinase C is a lipid-dependent protein kinase required for yeast's cell cycle and plays a role maintaining cell wall integrity (Choi et al., 2005). In mammalian cells protein kinase C plays a central role in the transduction of lipid second messengers generated by receptor-mediated

hydrolysis of membrane phospholipids. Phosphorylation of choline kinase by protein kinase in *S. cerevisiae* may represent a mechanism by which lipid signaling transduction pathways are coordinately regulated to phosphatidylcholine synthesis and cell growth (Figure 7).

2. Transcriptional regulation of choline kinase

2.1. Transcriptional factors that are involved in choline kinase expression

2.1.1. Activator protein 1 (AP-1)

The activator protein 1 (AP-1) is a heterodimeric transcription factor composed of c-Fos protein, c-Jun protein, activating transcription factor (ATF) and jun dimerization protein (JDP) (Hess et al., 2004). These transcription factors in the complex interact via their leucine-zipper domains, which in turn bring together their basic domains to bind DNA in a sequence-specific manner. AP-1 regulates transcription of genes by binding to a promoter region containing 12-*O*-tetradecanoylphorbol 13-acetate (`TPA'; PMA)-responsive element (TRE; 5'-TG/TAG/CTCA-3'). Different DNA sequence elements are preferentially recognized depending on the composition of the AP-1. For example, AP-1 (c-Fos/c-Jun) binds to 5’-TGAGTCA-3’ whereas AP-1 (ATF/c-Jun) binds to 5’-TTACCTCA-3’. AP-1 regulates gene expression in response to a variety of stimuli, including cytokines, growth factors, stress, and bacterial and viral infections. AP-1 in turn controls a number of cellular processes including differentiation, proliferation, and apoptosis (Florin et al., 2004).

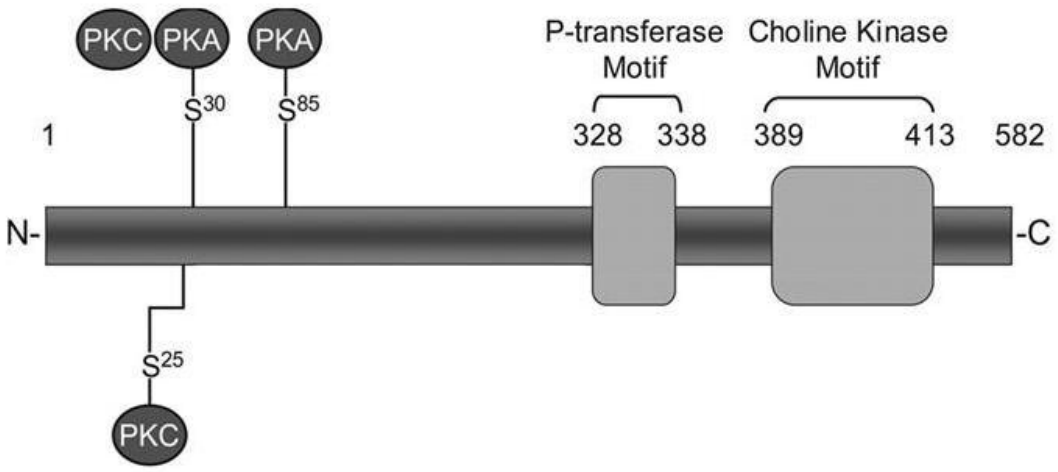

Figure 7. Domain structure of yeast choline kinase: The diagram shows the positions of the phosphotransferase (P-transferase) and choline kinase motifs and protein kinase A and C (PKA and PKC) target sites in the choline kinase protein sequence. The numbers on the top of the diagram indicate amino acid positions. Modified from Choi et al., 2005.

2.1.2. Hypoxia Inducible Factor (HIF-1)

The transcriptional factor hypoxia-inducible factor 1(HIF-1) plays an essential role in the adaptive response of cells to reduced oxygen tension (Semenza, 1998). It functions as a master regulator of responses to oxygen and undergoes conformational changes in response to varying oxygen concentrations. HIF-1 consists of α and β-subunits which are both helix-loop-helix transcription factors (Semenza, 2000). These subunits exist as a series of isoforms encoded by distinct genetic loci. The β-subunit is constitutively expressed and its' activity is controlled in an oxygen independent manner. Expression of the α-subunit is induced by cellular hypoxia and is maintained at low levels in most cells in normal oxygen tension. The induction of HIF-1α is a critical step in the hypoxic response and occurs via increased mRNA expression, protein stabilization, and nuclear localization. The levels of HIF-1α are the primary

determinant of HIF-1 DNA binding and transcriptional activity. HIF1 regulates expression of hypoxia responsive genes by binding to hypoxia response element (HRE), 5’-RCGTG-3’.

2.1.3 Sp/KLF transcription factor (SP-1)

Transcription factor Sp1 is a zinc-finger protein that binds GC-rich elements (Philipsen and Suske, 1999). Its zinc fingers are of the Cys_2/His_2 type and binds the consensus sequence 5'-(G/T)GGGCGG(G/A)(G/A)(C/T)-3' (GC box element). GC-rich sequences are common regulatory elements in promoters of housekeeping genes as well as many tissue-specific genes. Sp1 has traditionally been considered as a constitutive transcription factor regulating basal promoter activity because it is expressed in all cell types and Sp1-binding sites are found in the promoters of many housekeeping genes. However, it is becoming increasingly clear that Sp1 is also involved in tissue-specific gene expression, its activity being finely modulated by a variety of stimuli through multiple posttranslational modifications (Bouwman and Philipsen, 2002). Transcription factor Sp1 has recently been shown to be overexpressed in a number of human cancers and its overexpression contributes to malignant transformation. Sp1 regulates the expression of a number of genes participating in multiple aspects of tumorigenesis such as angiogenesis, cell growth and apoptosis resistance.

2.1.4. Cyclic AMP response element (CRE) -binding protein (CREB)

One of the best characterized stimulus-induced transcription factors, cyclic AMP response element (CRE) -binding protein (CREB), activates transcription of

target genes in response to a diverse array of stimuli, including peptide hormones, growth factors, and neuronal activity. These stimuli activate a variety of protein kinases including protein kinase A (PKA), pp90 ribosomal S6 kinase (pp90RSK), and Ca^{2+}/calmodulin-dependent protein kinases (CaMKs) (Shaywitz and Greenberg, 1999). All these kinases phosphorylates CREB at a particular residue, serine 133 (Ser133), and phosphorylation of Ser133 is required for CREB-mediated transcription response.

2.1.5 Xenobiotic response element (XRE) binding Aryl hydrocarbon receptor (AhR)/Hypoxia Inducible Factor

The Aryl hydrocarbon receptor (AhR or AHR) is a member of the family of basic-helix-loop-helix transcription factors. AhR is a cytosolic transcription factor that is normally inactive, bound to several co-chaperones. Upon ligand binding to chemicals such as 2,3,7,8-tetrachlorodibenzo-p-dioxin (TCDD), the chaperones dissociate resulting in AhR translocating into the nucleus and dimerizing with HIF1α (also known as AhR nuclear translocator), leading to changes in gene transcription. The classical recognition motif of the AhR/ HIF1α complex, referred to as xenobiotic- responsive element (XRE), contains the core sequence 5'-GCGTG-3' within the consensus sequence 5'-T/GNGCGTGA/CG/CA-3' (Lusska et al., 1993; Yao et al., 1992) in the promoter region of AhR responsive genes.

2.2. Regulatory mechanism responsible for ChKα gene expression

2.2.1. Promoter analysis of rodent ChKα gene

The promoter region of mouse and rat ChKα gene is highly conserved (Aoyama et al., 2004). In mouse liver-derived HePa-1 cells, promoter reporter assay identified 2 promoter regions upstream (distal and proximal) of ChKα. The distal promoter region of ChKα contained AP-1 binding site and xenobiotic response element (XRE, also known as PAH-response element), suggesting that in liver, exposure to CCl_4 or PAH could increase expression of choline kinase (Figure 8). The proximal promoter of ChKα contained 3 Sp-1 site and 1 CREB site. This is interesting as the next enzyme of CDP-choline pathway, CCT also has SP-1 sites in its proximal promoter. Presence of SP-1 sites in two regulatory enzymes might allow coordinated regulation of CDP-choline pathway by SP-1.

2.2.2. Promoter analysis of human ChKα gene

Recently, a putative promoter was isolated upstream of human ChKα gene (Glunde et al., 2008). Like the promoter isolated upstream of rodent ChKα gene, human ChKα promoter had a high GC content and was TATA less. No core promoter region was recognized. In their study, six putative hypoxia response elements (5'-CGTG-3') were identified out of which 4 closely spaced HREs (HRE 3-6) were shown to bind HIF1α (Figure 9). These 4 HRE sites were found to be associated with up-regulation of ChKα expression in promoter-reporter assays under hypoxic condition.

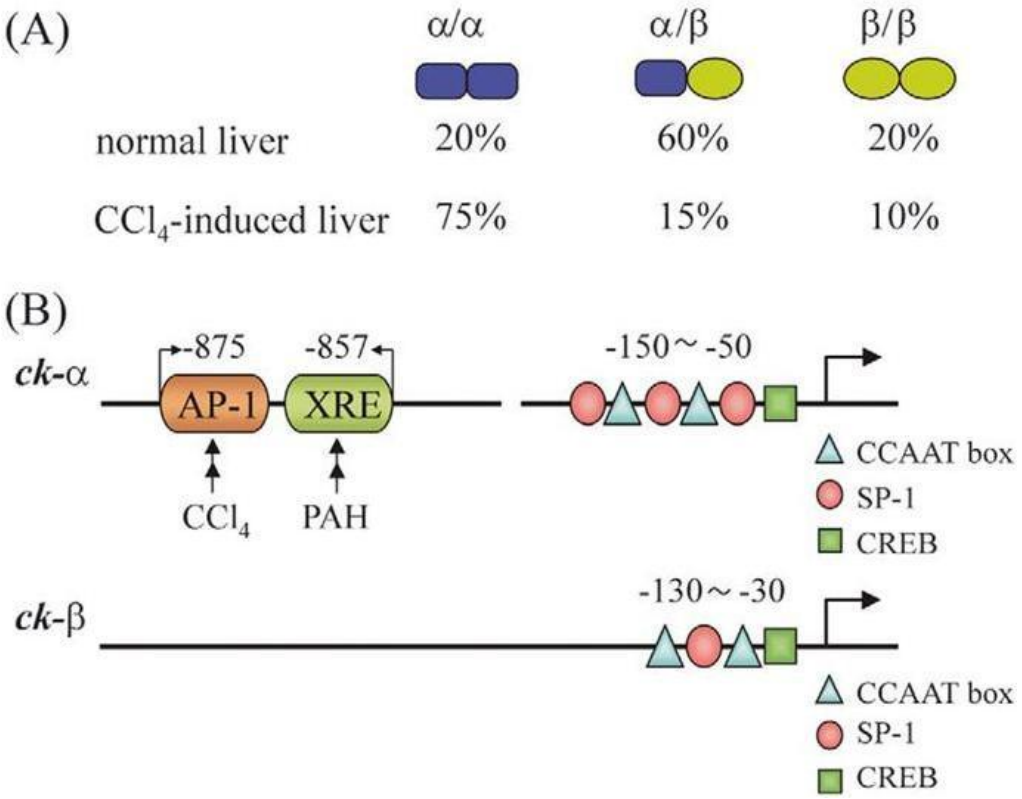

Figure 8. Effect of CCl_4 treatment on expression of choline kinase in rat liver (A), and (B) schematic diagram of upstream promoter of rodent choline kinase showing presence of AP-1 binding site in choline kinase a promoter. Modified from Aoyama et al., 2004.

Figure 9. Schematic diagram of promoter region upstream of human choline kinase α gene. Figure shows putative 6 HRE sites. Modified from Glunde et al., 2008.

3. Choline transport and metabolism in normal and cancer cells

3.1 Choline transport in normal cells

Choline transport is required for functioning of the CDP-choline pathway. However, since choline is a charged hydrophilic cation, transport mechanisms are required for it to cross biological membranes. Three types of transport mechanisms have been reported based on sodium dependency, Km for choline and Ki for hemicholinium (specific inhibitor of choline transport) (Lockman and Allen, 2002). Transport mechanisms include: 1. Sodium-dependent high-affinity uptake mechanism (Lockman and Allen, 2002) found in synaptosomes (choline Km < 10 µM ; hemicholinium Ki ~ 0.001-0.1 µM); 2. Sodium- independent low-affinity uptake mechanism (Lockman and Allen, 2002) found ubiquitously in all cells (choline Km > 30 µM ; hemicholinium Ki ~ 100 µM); and 3. A unique choline uptake mechanism found in blood-brain barrier choline transport that has affinity for choline similar to high affinity mechanism but sodium independence, and hemicholinium Ki similar to low affinity mechanism (Lockman and Allen, 2002).

3.2. Choline transport in cancer cell lines and cancerous tissues

Elevated choline tracer levels seen in the tumors have been postulated to be dependent on high choline kinase activity seen in tumors (Katz-Brull and Degani, 1996; DeGrado et al., 2001; Hara et al., 2002; Katz-Brull et al., 2002). However, elevated choline tracer levels in tissues would also require increased transport of choline. A non-metabolizable [^{18}F]fluorinated choline analog, deshydroxy- [^{18}F]fluorocholine ([^{18}F]dOC) was used by Henrikson et al. to address choline transport in cancer cells (Henriksen et al., 2004). Concentration-

dependent inhibition of membrane transport of both compounds by similar concentration of cold choline showed involvement of choline specific transport system in transporting [^{18}F]dOC into cultured rat pancreatic carcinoma (AR42J) cells (Henriksen et al., 2004). Uptake of [^{18}F]dOC was compared with that of [^{11}C]choline in cultured rat pancreatic carcinoma (AR42J) and PC-3 human prostate cancer cells at different time points. In the study, the fraction of [^{18}F]dOC in PC-3 and AR42J cells after 5 min incubation time was comparable to that of [^{11}C]choline, whereas the uptake of [^{11}C]choline was more after 20 min incubation time as compared to [^{18}F]dOC . The results from the experiments with cultured cell lines showed that, at early time points after incubation (5 min), transport seems to be the limiting factor with minimum effect of phosphorylation (Henriksen et al., 2004). At late time points (20 min), phosphorylation was important for retention of choline. Uptake of radiolabeled choline at the time relevant for oncological PET (Positron Emission Tomography) is likely dominated by choline transport although dual time PET is dependent also on choline kinase activity via metabolic trapping (Henriksen et al., 2004). In dual time PET, choline retention is measured at two time points. Increased choline retention with time is primarily due to preferential uptake and phosphorylation of choline in tumor as compared to normal cells.

Choline transport in cancer cells is at present not well understood due to limited data on choline transporter in cancer cells. The identity of the transporter for choline in cancer cells is unknown, although recent work (Martel et al., 2001) has identified two sodium independent 1-methyl-4-phenylpyridinium (MPP^+)

transporters in colon adenocarcinoma cells. These transporters belong to the amphiphilic solute facilitator (ASF) family that include recently identified (and cloned) choline transporter hOCT1 (Burckhardt and Wolff, 2000) and hOCT3 (Burckhardt and Wolff, 2000) in kidney and liver. Saturation kinetics and substrate specificity of choline transport in many cancer cell line have shown similarity to organic cation transporters (OCTs) reported in kidney and liver. In future, identification, cloning and characterization of choline transporters in cancer cells will lead to better understanding of their role in carcinogenesis.

3.3 Choline metabolism

Choline, after entering the cell, can either be oxidized to betaine by mitochondrial enzymes mostly seen in liver or kidney or converted to phosphocholine by cytosolic choline kinase. Metabolites of choline have different roles. In liver, betaine is an important donor of methyl group to homocysteine for the formation of methionine (Finkelstein et al., 1982). In kidney, betaine serves as an osmolyte (Garcia-Perez and Burg, 1991).The major pathway of choline incorporation into phosphatidylcholine in mammalian cells (other than liver and kidney) is via CDP-choline pathway. Choline can also be retained in the cells in free choline form as seen in human mammary epithelial cells (HMECs) (Katz-Brull et al., 2002).

Choline kinase is known to be overexpressed in lung, colorectal and prostate cancers (Ramirez de Molina et al., 2002) and in human mammary carcinomas (Ramirez de Molina et al., 2002). Most of the choline in MCF7 cells (breast cancer cell line) was converted to phosphocholine and then routed

through the CDP-choline pathway to form choline phospholipids. A significant amount of choline (~25%) was oxidized to betaine, and most of betaine was found in the growth medium of the cells. It therefore appears that the two pathways, phosphorylation and oxidation of choline, are both augmented in the course of malignant transformation of mammary cells (Katz-Brull et al., 2002).

4. Choline kinase as an oncogene

4.1. Choline kinase and cell signaling

It has been shown that phosphocholine confers mitogenic properties to mouse fibroblasts upon stimulation by PDGF or FGF (Cuadrado et al., 1993; Jimenez et al., 1995). A full understanding of how choline kinase and its downstream substrates contribute to tumorigensis has yet to be disclosed, although some previous studies clearly correlate choline kinase regulation with Rho A signaling, and transcriptome analysis of choline kinase overexpression demonstrates its effects on cell cycle regulation and apoptosis impairment (Rodriguez-Gonzalez et al., 2004; Ramirez de Molina et al., 2005; Ramirez de Molina et al., 2008). Recently, using a human siRNA library, various kinases were silenced in MDA-MB 468 breast cancer cells to screen for candidate kinases that regulate Akt phosphorylation (Chua et al., 2009). In the study, ~ 12% of the human kinome could directly or indirectly regulate Akt(ser473) phosphorylation. Silencing of ChKα reduced Akt(ser473) phosphorylation significantly, suggesting the potential role of ChKα as a regulator of Akt pathways.

4.2. Choline as a cancer biomarker

4.2.1. Choline based Positron Emission Tomography (PET) imaging of malignant cancers

High choline uptake and increased choline kinase activity have been reported in many cancers (Katz-Brull and Degani, 1996; DeGrado et al., 2001; Hara et al., 2002; Katz-Brull et al., 2002). Choline kinase is known to be over-expressed in lung, colorectal, and prostate cancers (Ramirez de Molina et al., 2002). The potential for PET imaging using [^{11}C]choline has been shown in detection of brain tumor (Hara et al., 1997; Shinoura et al., 1997), prostate carcinoma (Hara et al., 1998), and esophageal carcinoma (Hara, 1987). However, the short half-life of [^{11}C]choline ($T_{1/2}$ = 20 min) limits its use to facilities that have a cyclotron within a short distance from the imaging suite. To allow for more practical distribution of a longer-lived tracer, the ^{18}F-labeled choline analog ($T_{1/2}$ = 109 min), [^{18}F]fluorocholine ([^{18}F]FCH) was developed (DeGrado et al., 2001; DeGrado et al., 2001). Preliminary studies have shown [^{18}F]FCH to be a promising PET imaging tracer for prostate cancer, hepatocellular carcinoma and brain tumor imaging (Coleman et al., 2000; DeGrado et al., 2001; Hara, 2001; Price et al., 2002; Kwee et al., 2004; Kwee et al., 2005; Schmid et al., 2005; Cimitan et al., 2006; Heinisch et al., 2006; Kwee et al., 2006; Talbot et al., 2006) .

4.2.2. Choline based Magnetic Resonance Spectrometry Imaging (MRSI) of malignant cancers

High resolution ^{1}HMR spectroscopy (MRS) of tissue and cell extracts can resolve individual choline phospholipid metabolites and can be used to quantify

phosphocholine (PC), glycerophosphocholine (GPC), and free choline (Cho)(Ackerstaff et al., 2003). With ^{1}H-MRS of intact cells or solid tumors, an unresolved signal of overlapping PC, GPC, and free choline resonances, referred to as total choline containing metabolites (tCho) is observed. The elevation of the tCho signal detected in preclinical and clinical ^{1}H magnetic resonance spectroscopy (MRS) and MRS imaging (MRSI) studies (Glunde et al., 2008) is often observed to be associated with malignancy and high rate of angiogenesis. In prostate cancer, this tCho signal, combined with the citrate signal, has been shown to correlate with staging of the disease by the Gleason score and has shown promise in clinical 1H MRSI studies of prostate cancer to noninvasively evaluate prostate cancer aggressiveness (Glunde et al., 2008).

5. Specific aims and hypotheses

The goals for this thesis were: (a) to confirm if hypoxia mediated decrease in choline phosphorylation and choline kinase activity is a universal response in cancer cells, (b) to understand the mechanism behind inhibition of choline phosphorylation in hypoxic cells and (c) to understand the effect of hypoxia and increased choline kinase activity on malignant phenotype of cancer cells.

Three hypotheses were examined in this study:

Hypothesis 1*: Choline phosphorylation and retention is decreased in hypoxic cancer cells and hypoxic tumor xenograft model.*

Aim 1: Evaluate fate of choline in hypoxic cancer cells and in subcutaneous 9L glioma tumor xenograft model.

Hypothesis 2*: Decreased choline phosphorylation in hypoxic prostate cancer cells is due to HIF1 mediated transcriptional control of* ChKα*.*

Aim 2a: Evaluate ChKα.and HIF1α*.* expression in cancer cells exposed to normoxia (21% O_2) and hypoxia (1% O_2) for 24h and 48h.

Aim 2b: Determine whether modulation of choline uptake and choline kinase activity is a HIF1α dependent response.

Aim 3b: Characterize the ChKα promoter associated with HIF1α mediated regulation of ChKα expression.

Hypothesis 3*: Hypoxia and over-expression of choline kinase influences malignant phenotypes of prostate cancer cells representing different stages of disease progression.*

Aim 3: Evaluate affects of hypoxia and over-expression of choline kinase on proliferation, migration, invasion and colony formation of non-invasive LNCaP cells and highly invasive PC-3 cells.

CHAPTER I

Choline phosphorylation and retention is decreased in hypoxic cancer cells and the hypoxic tumor xenograft model

1. Abstract

The choline kinase enzyme is frequently over-expressed in malignancy. Therefore, choline, which is a substrate for choline kinase, has the potential to serve as oncologic probe for imaging cancers. Effect of hypoxia on choline uptake and metabolism in cancer cells was examined as a test of the hypothesis that tumor oxygenation should be considered when choline based imaging studies are used to noninvasively detect malignant cells. This hypothesis was tested by exposing cancer cells to low oxygen environment (1% O_2) for 24h. Hypoxia had a negative impact on choline uptake and phosphorylation in rat 9L glioma cells, human PC-3 and LNCaP prostate cancer cells. To further test this response in *in vivo* model, choline uptake and metabolism was examined in hypoxic subcutaneous 9L tumor. Uptake of choline was transient in the hypoxic 9L tumor and the majority of radiolabel in tumor, like in hypoxic cultured 9L cells, was found as nonmetabolized choline. Previously, [^{18}F]Fluorocholine (FCH) has been developed as an analog of choline for tumor imaging. Regional FCH deposition and tumor perfusion study with the 9L glioma tumors showed that FCH uptake spatial pattern followed closely with the intratumoral distribution of perfusion. No significant change was seen with time in average blood flow in these hypoxic 9L tumors but there was a significant decrease in average FCH

retention from 5 min to 20 min. The study suggests that the heterogeneity of tumor uptake of choline analogs depends largely on the heterogeneity of perfusion/oxygenation and should be carefully considered in interpreting choline based imaging.

2. Introduction

In recent years, choline metabolites have been widely studied in cancer research. High choline uptake and increased choline kinase activity have been reported in lung, breast, colorectal, and prostate cancers (DeGrado et al., 2001; Katz-Brull et al., 2002; Ramirez de Molina et al., 2002). This alteration in choline metabolism in neoplasm relative to normal tissues has motivated evaluation of proton magnetic resonance spectroscopic imaging (MRSI) of total choline pool size (Jacobs et al., 2004; Katz-Brull et al., 2002) and positron emission tomography (PET) imaging of choline uptake (DeGrado et al., 2001; Shinoura et al., 1997) as cancer imaging techniques for diagnosis and therapy monitoring.

Although overall choline uptake in tumors is high, intra-tumoral uptake pattern regions can exhibit considerable heterogeneity (Jacobs et al., 2004; Schmid et al., 2005). Multiple factors may be involved, such as heterogeneity of tumor perfusion, oxygenation (hypoxia) and extracellular pH. Such factors are known to regulate biochemical and physiological processes within tumor cells (Kallinowski et al., 1989) but their effects on choline metabolism are not well understood. Tracer studies with mouse atrial cardiomyocyte tumor lineage, AT-1 (Sarri et al., 2006) showed that hypoxic exposure reduces choline

uptake/phosphorylation (Figure 10). Reduced tracer uptake was accompanied by reduced choline kinase activity.

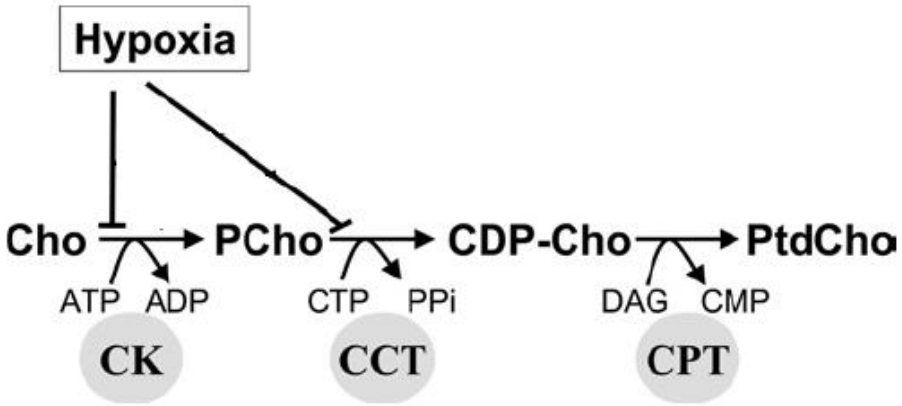

Figure 10. Hypoxia inhibits phosphorylation of choline and formation of CDP-choline in atrial cardiomyocytes. Modified from Sarri et al., 2006.

This effect of hypoxia on choline uptake/metabolism was not limited to cancer cells derived from rodents but also seen in human cancer cell lines. In our previously reported study, with two human prostate cancer cell lines after 4h of anoxia (0% O_2), PC-3 cells showed 15% decrease in choline uptake, whereas LNCaP cells showed 28% decrease in choline uptake (Figure 11) (Hara et al., 2006). After 24h of anoxia, choline uptake and cell proliferation rate continued to decrease in both cell lines with no change in cell viability. The purpose of this study was to evaluate the effect of chronic hypoxia (1% O_2) on choline uptake and metabolism in cancer cells.

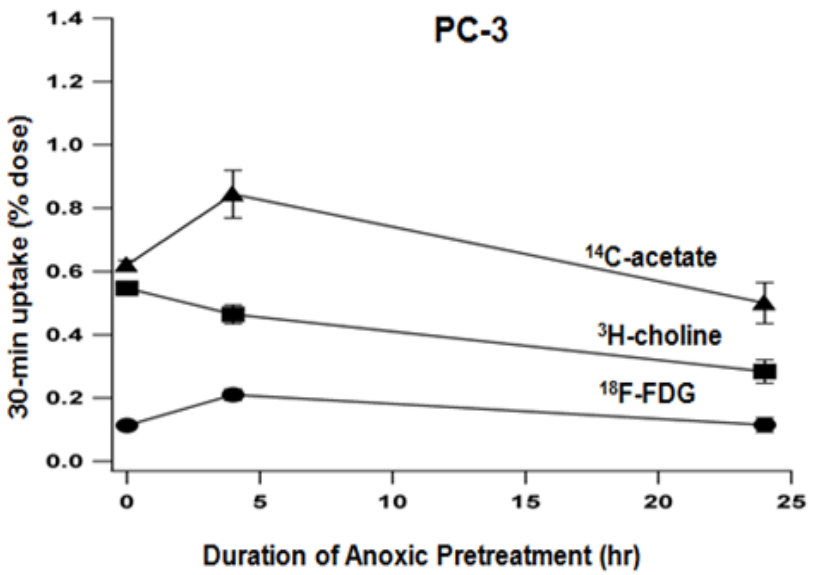

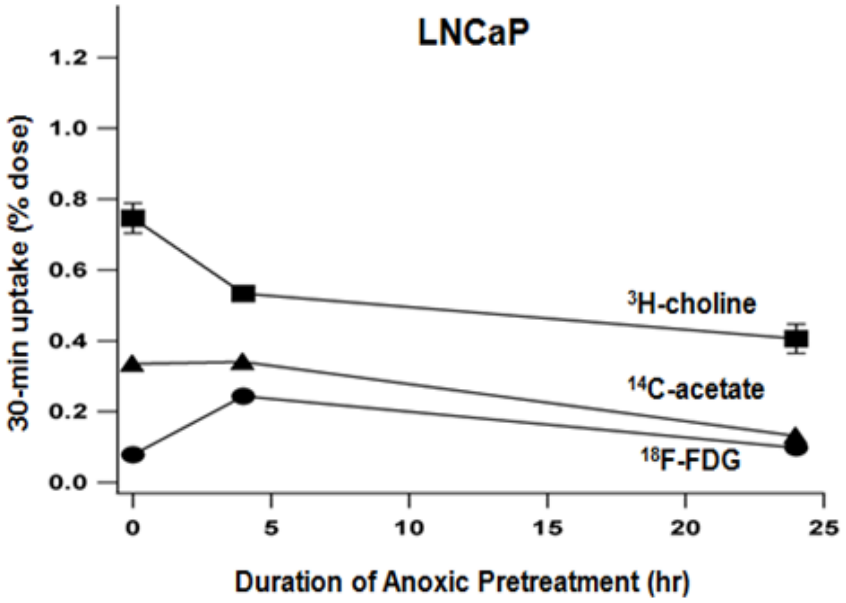

Figure 11. Uptake of [^{3}H]choline, [^{14}C]acetate and [^{18}F]FDG in prostate cancer cells: (A) and LNCaP cells (B) in normal-serum-supplemented medium. The 30-min uptake was measured after 0, 4 and 24 h of anoxic incubation, without interrupting anoxia. Error bars indicate standard deviations (*n* = 5). Modified from Hara et al., 2006.

3. Materials and Methods

3.1. Material chart

ATCC, Manassas, VA	9L glioma cells PC-3 and LNCaP prostate cancer cells RPMI-1640 medium PBS Fetal bovine serum 0.25% Trypsin-EDTA
Charles River Laboratoires, Wilmington, MA	Male Fisher CDF 344 rats
Perkin Elmer, Waltham, MA	Solvable
Eppendorf, Westbury, NY	Centrifuge 5415R
Sigma, St. Louis, MO	Sodium Pentobarbital, Streptomycin, NaOH, SDS, RIPA lysis buffer, protease inhibitor cocktail, DMOG, chloroform, methanol, urea, sulfiuric acid, acetonitrile, ammonium acetate, penicillin, scintillation cocktail, glacial acetic acid, HEPES , Triton X-100, EDTA, Bovine Adult Serum, N-tosyl-Lphenylalanine chloromethyl ketone (TPCK), trypsin inhibitor, leupeptin, DTT, PMSF), Tris, HCl, ATP, $MgCl_2$, choline
Grace (Alltech), Deerfield, IL	HPLC column, column heater
Varian, Palo Alto, CA	Mass-spectrometer
Research Products International Corp., Prospect, IL	Polytron homogenizer
Waters, Milford, MA	HPLC system
Ruskinn Technologies, Bridgend, UK	Invivo work station
GE Healthcare (Amersham Biosciences), Piscataway, NJ	[^{14}C]choline, [^{14}C]iodoantipyrine (IAP) and [^{3}H]choline

3.2. Tumor xenograft model

Male Fisher CDF 344 rats (~ 200 g) were anesthetized with sodium pentobarbital (45 mg/kg IP). The thigh area was shaved and 2-3 x 10^6 cultured 9L glioma cells suspended in 50 µl PBS were inoculated under the skin. The tumor was allowed to grow to the size of approximately 1.5 cm^3 (about 4 weeks).

3.3. Establishment of hypoxic environment

Cells were cultured in high glucose (4.5g/L) RPMI-1640 medium (ATCC) or DMEM (ATCC) supplemented with 10% (v/v) fetal bovine serum (ATCC), 100 units/ml penicillin (SIGMA), and 0.1 mg/ml streptomycin (SIGMA). Cells were grown at 37°C in a humidified CO_2 incubator. For hypoxic conditions, cells in medium were exposed to 1% O_2 balanced with 5% CO_2/94% N_2 in a hypoxia work station (In vivo$_2$ 300, Ruskinn Technologies, Bridgend, UK) for 24h. For chromatin immunoprecipitation (ChIP) assays and promoter-luciferase assays, hypoxic conditions were induced by exposing cells to 2mM dimethyloxaloylglycine (DMOG) for 24h. DMOG stabilizes HIF1α and acts as a hypoxia mimetic.

3.4. Uptake of radiolabeled choline in cancer cells

Studies of tracer choline uptake were performed in cultured cancer cells in normoxic and hypoxic conditions. For the latter condition, a 24 h exposure to hypoxia (1% O_2) was chosen as a preconditioning period before administration of choline radiotracers because significant changes in protein expression are seen only during prolonged (>16 h) hypoxic (1% O_2) exposure (Liu et al., 2006).

Furthermore, in our experience, cancer cells are viable under hypoxia (1% O_2) for 48 h (Hara et al., 2006). Sub-confluent cultures of cancer cells were placed under a humidified normoxic gas mixture (21% O_2, 75% N_2, 5% CO_2) or a hypoxic gas mixture (1% O_2, 94% N_2, 5% CO_2). After 24h incubation at 37°C, the cells were then incubated with radiolabeled choline for different time points. At the end of incubation, the cells were washed 3 times with chilled phosphate buffered saline (PBS). Exposure to respective gas mixture was maintained throughout the experiment. Uptake studies were done in cell medium supplemented with 10% fetal bovine serum in triplicate in 6 well plates. The medium contained 28 μM choline (physiological range 10-30 μM, ~ 74 KBq radiolabeled choline per well. After incubation with the radiotracers, the cells were lysed in 1 ml of 0.3 N NaOH and 1% SDS. Scintillation fluid was added to the samples and they were counted for ^{14}C-radioactivity using a liquid scintillation counter. For metabolite analysis, the cells were incubated with ~ 444 KBq radiolabeled choline per well.

3.5. Pulse chase experiment

To investigate the efflux rates of radioactivity from cancer cells a pulse chase experiment was performed. After 24 h incubation at 37°C under normoxic or hypoxic conditions, the cancer cells were incubated with radiolabeled choline for 2 h at 37°C under similar conditions. The cells were then washed with PBS and incubated in fresh medium. The cycle of washing and incubation was repeated every 15 min over a 2 h period. Radioactivity was counted in the PBS washes and the incubation medium after each cycle. The PBS washes and the fresh medium were equilibrated with 21% O_2 (normoxic condition) or 1% O_2

(hypoxic condition). Hydrophilic choline metabolites in the washout were analyzed using HPLC.

3.6. Measurement of choline metabolite levels in cells

For metabolite analysis, the cells were scraped in 500 µl chloroform/methanol (2:1) and sonicated at 4°C. To the sonicated cell suspension was added 100 µl aqueous urea (40%) and 100 µl sulfuric acid (5%). The cells were sonicated for another 15 s, and then centrifuged at 2,500 g for 5 min at 4°C. Hydrophilic choline metabolites in the aqueous layer were analyzed using gradient HPLC as described below. Aqueous and organic fractions were separated and counted.

3.7. Uptake of radiolabeled choline in tumor xenograft

Groups of animals (n = 4 each) were studied after bolus intravenous administration of [^{14}C]choline (1.8 MBq) and [^{18}F]FCH (5 MBq) in isotonic saline. At 5 or 20 min after bolus injection, rats were euthanized and blood samples/tumor tissues/skeletal muscle was excised for radioactivity counting and metabolite analysis. Tumor and skeletal muscle tissue samples were rinsed in chilled saline and blotted to remove excess liquid. A portion of each tissue was weighed and counted for radioactivity, while the remainder was used for metabolite analysis. For calculating uptake of tracers, ^{18}F radioactivity was counted immediately. For ^{14}C-radioactivity, ^{18}F-radioactivity was allowed to decay while tumor tissue or muscles are incubated with 0.5 ml tissue solubilizer (SOLVABLE, Perkin Elmer) at 37°C overnight, 5 ml scintillation cocktail was added, and ^{14}C-radioactivity was counted.

3.8. Analysis of radiolabeled choline metabolites in cancer cells and tumor tissue

Tissue samples were homogenized using a polytron homogenizer in 5 ml chloroform/methanol (2:1) at 4°C. The homogenate was sonicated for 15 s, then 1 ml aqueous urea (40%) and 1 ml sulfuric acid (5%) was added. The suspension was sonicated for another 15 s. The suspension was centrifuged at 2,500 g for 5 min. Aqueous and organic fractions were separated and counted. Plasma samples were worked up as described above for tissue without homogenization. Samples of the aqueous phase were applied to an Adsorbosphere Silica HPLC column (4.6 x 250 mm, 10 μ) (Alltech Associates, Deerfield, IL). The following gradient was used for the HPLC separation: Solvent B in the eluent: 0% at 0-3 min, 0-30% at 3-10 min, 30-40% at 10-20 min, 40-100% at 20-22 min, 100% at 22-50 min, 100-0% 50-56 min, and 0% at 56-57 min. Solvent A was acetonitrile/water/ethanol/ 1M ammonium acetate/glacial acetic acid (0.8/0.127/0.068/0.003/0.002 (v/v)) and Solvent B was Acetonitrile/water/ethanol/1M ammonium acetate/glacial acetic acid (0.44/0.44/0.085/0.027/0.018 (v/v)). The HPLC eluant was collected in 1-min fractions. Based on their retention time, the metabolites phosphocholine (31 min), phosphoryl-[^{18}F]FCH (28 min), choline (16 min), betaine (11 min), [^{18}F]FCH (13 min) and [^{18}F]fluorobetaine (8 min) were identified in the fractions. Retention times were determined using unlabeled standards of choline, FCH, betaine, fluorobetaine, phosphocholine and phosphoryl-FCH and mass-spectrometry detection (Varian, Palo Alto, CA). ^{18}F-radioactivity in 100 μl standard of injectate

and collected samples were measured in gamma counter. The samples were then allowed to decay for at least 24 h. The injectate and samples in a liquid scintillation counter were counted for ^{14}C-radioactivity.

3.9. Measurement of choline kinase activity in cancer cells and tumor tissue

The cells were scraped and homogenized in chilled extraction buffer pH 7.5 (30 mM HEPES pH 7.5, 3% Triton X-100, 2 mM EDTA, 2% Adult Bovine Serum, 10 μM N-tosyl-Lphenylalanine chloromethyl ketone (TPCK), 10 mg/ml trypsin inhibitor, 1 μM leupeptin, 0.75 mg/ml DTT, 0.4 mg/ml PMSF). The cell homogenate was centrifuged for 10,000 g for 20 min at 4°C. The supernatant was used for the assay as described by (Ishidate and Nakazawa, 1992) . The assay mixture (300 μl) contained 0.1 M Tris-HCl, pH 7.5, 10 mM ATP, 12 mM $MgCl_2$, 100 μM choline, [^{14}C]choline (~ 0.7 MBq / assay mixture). Samples were incubated at 37°C for 30 min.

3.10. Tumor perfusion assay and spatial localization of radiolabeled choline in tumor xenograft

Regional FCH deposition and tumor perfusion were compared at sub millimeter spatial resolution by 2-D autoradiography of $^{18}F/^{14}C$ following administration of FCH and the perfusion marker, [^{14}C]iodoantipyrine (IAP). Tumors were excised, frozen at 5 min and 20 min after bolus administration of FCH. Intravenous infusion of IAP began 1 min prior to termination of experiment. The frozen tumor was sliced at 10 micron thickness. Quantitative maps of regional perfusion and FCH retention were obtained.

3.11. Statistical analysis

Results are presented as means ± standard deviation. Student's t-test was applied for statistical evaluation and a p-value <0.05 was considered significant.

4. Results

4.1. Hypoxia decreased choline uptake and phosphorylation in cancer cells

In normoxic cancer cells incubated with radiolabeled choline, the choline tracers were taken up avidly, and rapidly phosphorylated. The uptake of choline increased in a linear fashion with increasing incubation time in normoxic cancer cells (Figure 12-13). The aqueous soluble radioactivity was nearly completely (>95%) in the form of phosphocholine at incubation periods as short as 5 min. At 120 min, 99% of the radioactivity is contributed by phosphorylated form. The pattern of choline uptake and phosphorylation was different in hypoxia depending on the cancer cell. In hypoxic condition, majority of fraction at early time points <20min , was dominated by non-metabolized choline. At 120 min, following exposure to chronic hypoxia, two responses were seen. In one set of cancer cells (PC-3, prostate cancer cells), there was a significant difference in choline uptake at 120 min of incubation primarily due to strong inhibition of choline phosphorylation (Figure 12). At 120 min, most of the radioactivity (98%) in these cells is contributed by non-metabolized choline with <2% in phosphocholine form. In the second set of cancer cells (9L glioma cells and LNCaP, prostate cancer), choline phosphorylation was decreased in hypoxia but not to the extent seen in PC-3 and ovarian cancer cells. This slight but significant decrease in choline phosphorylation caused a modest decrease in choline retention at 120 min of

incubation (Figure 13). The major proportion (95%) of the radioactivity in these cells is contributed by phosphorylated form at 120 min incubation.

To further investigate the fate of radiolabeled choline metabolites, a pulse-chase experiment was performed. Two cell lines were chosen representing the two uptake/phosphorylation responses to hypoxia. For strong choline phosphorylation inhibition response, PC-3 cells were used and for the modest choline phosphorylation inhibition 9L glioma cells were used. After administering a pulse of radiolabeled choline tracers for 120 min in normoxic condition, moderate levels of radioactivity were washed out of PC-3 and 9L glioma cells in successive 15 min incubations (Figures 14 and 15). In PC-3 cells, the washout rate was significantly higher in hypoxia as compared to normoxia (Figure 14). While in case of 9L glioma cells, the difference between washout rates in hypoxia was significantly higher than seen for normoxic cells (Figure 15).

4.2. Hypoxia increased choline/phosphocholine ratio in cancer cells

To further confirm the significant decrease in choline phosphorylation in PC-3 cells, steady state levels of choline metabolites were measured. In the normoxic state, PC-3 cells had 0.031 ± 0.012 µmol choline /200mg protein and 2.1 ± 0.2 µmol phospho-choline /200mg protein. Marked changes in concentrations of these metabolites were seen in the hypoxic state. Hypoxia caused a ~ 666% increase in concentration of choline and 14% decrease of phosphocholine (Table 2). Consistent with the decreased choline phosphorylation, a 30% decrease in choline kinase activity was observed in hypoxic cells (Table 2). Hypoxia also decreased the energy state of PC-3 cells as

evidenced by ~ 19% reduction in concentration of ATP. The phosphocholine/choline ratio was decreased by 10 fold in hypoxic cells (phosphocholine/choline = 7.8) as compared to normoxic cells (phosphocholine/choline = 70) (Table 3). The MAR/Keq of choline phosphorylation in PC-3 was 19 X 10^{-4} based on published Keq value = 1.24 X 10^{4} (Infante, 1977, Infante et al., 1978).

Table 3. Choline kinase (ChK) activity and metabolite levels in prostate cancer cell extracts in serum-supplemented medium after 24 h normoxia (1% O_2) and hypoxia (21% O_2) (n = 3, each condition). ChK activity is expressed as nmol choline phosphorylated/min/mg protein.*p<0.05 s values in normoxia using unpaired t-test.

Cell line	ChK activity	Choline mM	Phosphocholine mM	ATP mM
PC-3 Normoxia	2.43 ± 0.02	0.031 ± 0.012	2.1 ± 0.2	3.2 ± 0.2
PC-3 Hypoxia	1.7 ± 0.1*	0.23 ± 0.06*	1.8 ± 0.1*	2.6 ± 0.1*
LNCaP Normoxia	1.22 ± 0.04	0.031 ± 0.01	2.7 ± 0.1	4.4 ± 0.3
LNCaP Hypoxia	0.85 ± 0.1*	0.08 ± 0.02*	2.4 ± 0.1*	3.8 ± 0.2*

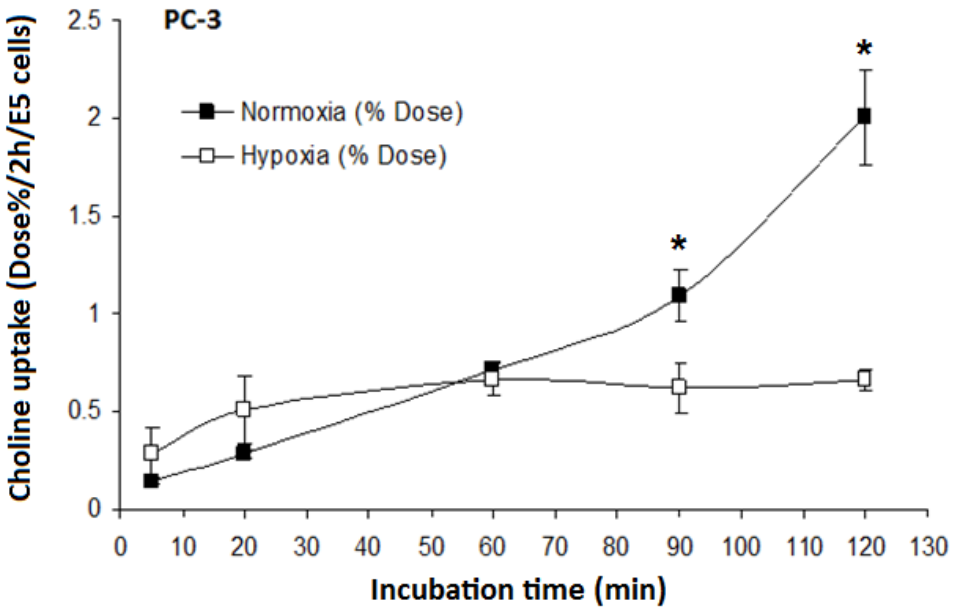

Figure 12. Uptake of radiolabeled choline in PC-3 prostate cancer cells. Uptake is shown as function of oxygenation status and incubation period. Values are shown as % administered dose per 10^6 cells (mean, n = 3). * $p < 0.05$ Vs values in normoxia using unpaired t-test.

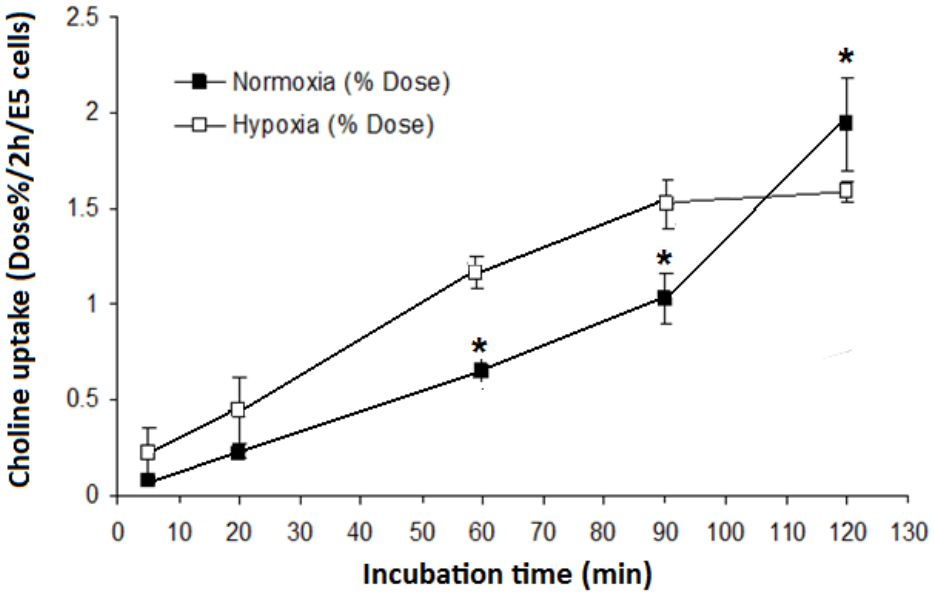

Figure 13. Uptake of radiolabeled choline in LNCaP prostate cancer cells: Uptake is shown as function of oxygenation status and incubation period. Values are shown as % administered dose per 10^6 cells (mean, n = 3). * $p < 0.05$ Vs values in normoxia using unpaired t-test.

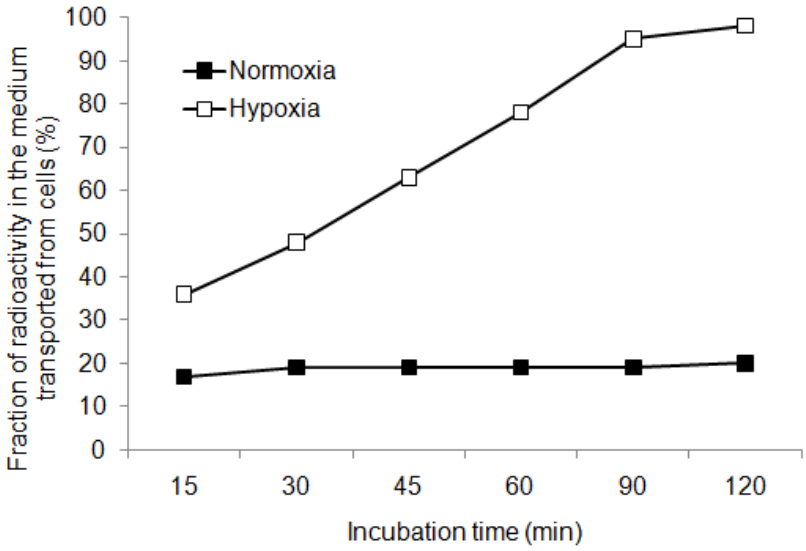

Figure 14. Efflux of choline radioactivity from normoxic and hypoxic PC-3 cells: Representative graph showing efflux of trapped choline radioactivity upon successive washing after incubating the cells for 2 h with [^{14}C]choline under normoxic (21% O_2) and hypoxic (1% O_2) condition.

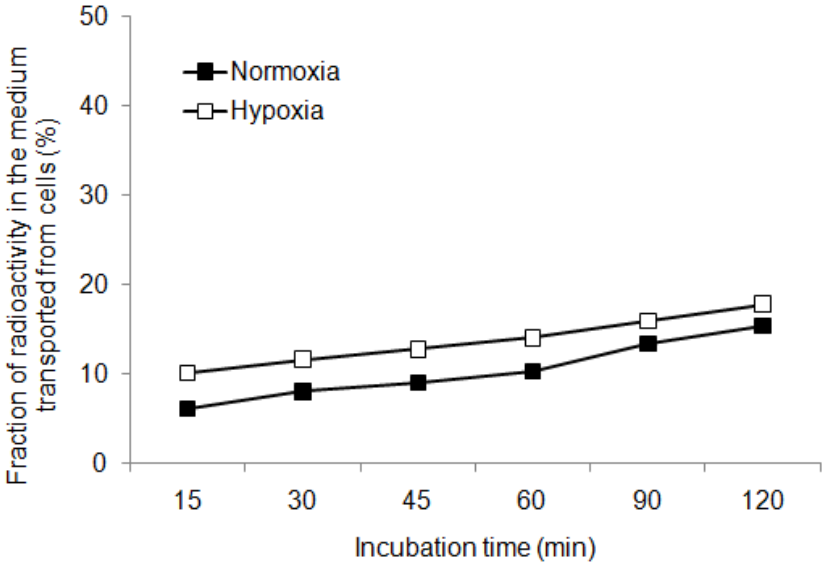

Figure 15. Efflux of choline radioactivity from normoxic and hypoxic 9L glioma cells: Representative graph showing efflux of trapped choline radioactivity upon successive washing after incubating the cells for 2 h with [^{14}C]choline under normoxic (21% O_2) and hypoxic (1% O_2) condition.

4.3. Uptake of radiolabeled choline in hypoxic subcutaneous tumor is transient

To understand the effect of hypoxia mediated inhibition of choline phosphorylation on choline uptake in animal tumor models, choline tracer studies were performed in hypoxic 9L glioma tumor model. In 9L tumor, hydrophilic metabolites dominated the fate of both [^{14}C]choline and [^{18}F]FCH, with 98% of radiolabel found in the aqueous phase at both 5min and 20min post-injection. Tumor: muscle and tumor: blood ratio decreased from 5 min to 20 min for both [^{14}C]choline and [^{18}F]FCH (Table 4). HPLC analysis of extracts of tumor showed major amount of radioactivity contributed by nonmetabolized [^{14}C]choline and [^{18}F]FCH. The fraction of nonmetabolized [^{18}F]FCH and [^{14}C]choline in tumor decreased from 5 min to 20 min. The fraction of radioactivity in the form of [^{14}C]betaine and [^{18}F]fluorobetaine was significantly small.

Table 4. Tumor- to-background ratio of [^{14}C]choline and [^{18}F]FCH in 9L-glioma bearing Fisher rat. Values are mean ± standard deviation (n = 4)

	Time post-injection (min)	^{14}C	^{18}F
Tumor : blood	5	4.22 ± 0.84	2.55 ± 0.66
	20	1.46 ± 1*	0.88 ± 0.58*
Tumor: muscle	5	5.85 ± 0.94*	6.27 ± 0.81
	20	1.05 ± 0.69*	1.05 ± 0.59*

*$p < 0.05$ Vs value at 5 min using unpaired t-test.

4.4. Choline uptake pattern coincides with blood flow pattern of the tumor xenograft

[^{18}F]FCH uptake pattern followed closely the intra-tumoral distribution of blood flow. The tumor had a necrotic center with no blood flow. The blood flow was restricted to the periphery of the tumor which coincided with the region that had appreciable [^{18}F]FCH retention (Figure 16). Transient uptake of [^{18}F]FCH in 9L tumor was confirmed evident from decrease in [^{18}F]FCH retention in the 9L tumor with time independent of blood flow (Table 5).

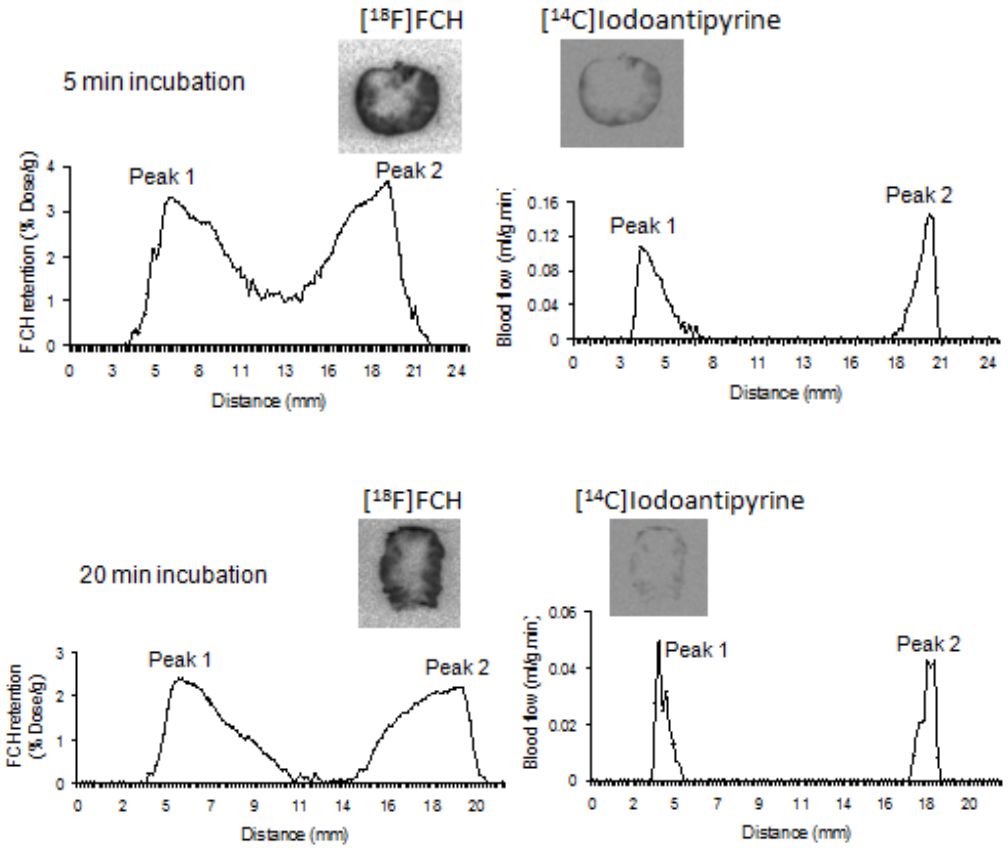

Figure 16. Representative autoradiograph of sections of 9L glioma tumors. [^{18}F]FCH retention correlated with blood flow marker [^{14}C]Iodoantipyrine at 5min and 20 min post-injection.

Table 5. Blood flow and FCH retention estimates of 9L glioma tumors at 5 min (n = 4) and 20 min (n = 4) post-injection.

Time post-injection (min)	Maximum blood flow (ml/g.min)	Average blood flow (ml/g.min)	Maximum FCH retention (% dose/g)	Average FCH retention (% dose/g)
5	0.17 ± 0.04	0.07 ± 0.028	3.27 ± 0.62	1.99 ± 0.32
20	0.11 ± 0.10	0.04 ± 0.032	2.14 ± 0.21*	1.102 ± 0.39*

*$p < 0.05$ Vs value at 5 min using unpaired t-test.

5. Discussion

Hypoxia decreased uptake of choline in all cancer cells studied. In some cells, the decrease was more pronounced than in others. In PC-3 cells, due to strong inhibition of choline phosphorylation, choline tracer accumulation was completely abrogated in hypoxic conditions for incubation periods greater than 20 min, whereas normoxic cells accumulated radiolabeled choline throughout a 2 h incubation period. Furthermore, the smaller amount of radiolabeled choline that was taken up by hypoxic PC-3 cells was quickly washed out when the medium did not contain radiotracer in the pulse chase experiment. In contrast, nearly all the radioactivity was retained within normoxic PC-3 cells in the form of radiolabeled phosphocholine. In 9L glioma cells, due to modest inhibition of choline phosphorylation, hypoxic 9L glioma cells were able to accumulate choline tracer with slower rate than seen in normoxic conditions. Due to slow choline phosphorylation, only modest levels of radioactivity were washed out of hypoxic 9L glioma cells as compared to normoxic cells. This washout rate was significantly less than that seen for hypoxic PC-3 cells.

The reason for the strong hypoxia-induced inhibition of choline uptake/ phosphorylation in PC-3 cells and ovarian cancer cells as compared to 9L glioma cells, LNCaP cells and pancreatic cancer cells is not clear. In both PC-3 and 9L glioma cells, choline kinase activity was decreased by 30% which contributed to decrease in choline phosphorylation in all hypoxic cells. The high Km of choline kinase for ATP and significant decrease in ATP levels in cancer cells could in part contribute to inhibition of phosphorylation in addition to reductions of choline kinase activity. Inhibition of choline phosphorylation due to ATP depletion was also reported in hypoxic HL-1 cardiomyocytes (Sarri et al., 2006) and AICAr treated hepatocytes (Jacobs et al., 2007). Pronounced decrease in choline phosphorylation in PC-3 and ovarian cancer cells as compared to other cells suggests that factors other than choline kinase and ATP may have a role in determining choline uptake and trapping. More work is needed to understand the mechanism of inhibition of choline phosphorylation in hypoxia in cancers.

To further confirm the results from tracer study for PC-3 cells, steady state concentrations of choline metabolites were measured. It was observed that PC-3 cells maintained a high ratio of steady-state concentrations of phosphocholine to choline irrespective of oxygenation status but hypoxia increased the steady-state choline concentration 10-fold while decreasing phosphocholine concentration by 15%. Increased steady-state choline/phosphocholine concentration ratio and decreased uptake and phosphorylation of exogenous radiolabeled choline in hypoxic PC-3 cells strongly suggest that hypoxia mediated inhibition of choline phosphorylation. This strongly supported the radiotracer studies.

It is well known that metabolites participating in rate-limiting metabolic reactions are regulated by modulation of associated catalyzing enzymes (Newsholme and Crabtree, 1973). A disequilibrium ratio (MAR/Keq) that is << 1 implies that the reaction be considered far from equilibrium or rate limiting. From this principle, Infante et al. showed that the reaction catalyzed by choline kinase is rate limiting in rat liver (Infante, 1977; Infante and Kinsella, 1978). Present study corroborates previous work showing that modulation of choline kinase can change concentration of choline metabolites in cancer cells.

Uptake of tracers in subcutaneous 9L tumor at 5 min and 20 min was dominated by choline radiotracers in their nonmetabolized form. This was in accordance with the inhibition of choline phosphorylation that was seen in hypoxic 9L glioma cultured cells. These results suggest that hypoxia can explain the low levels of choline phosphorylation in the 9L glioma tumor model. This notion is further supported by earlier reports demonstrating extreme levels of hypoxia (median pO_2 value 5.5-7 mm Hg (~ 1% O_2)) resulting from low perfusion in the same subcutaneous 9L tumor (Jenkins et al., 2000). Low perfusion rate and low choline retention rate was also confirmed by perfusion and choline retention quantitative maps generated from tumor sections. The results of choline tracer studies with cultured cancer cells and 9L glioma subcutaneous tumor may best interpolate to human tumors that are characteristically hypoxic. It follows that the utility of choline tracers in the clinical setting may be impacted by tumor hypoxia. Tumors that are hypoxic may exhibit low uptake of choline based tracers as governed by increased efflux of nonmetabolized tracer and decreased

metabolic trapping (phosphorylation). Thus, interpretations of clinical PET images with choline radiotracers should bear in mind that choline tracer uptake may underestimate tumor proliferation (or viability) in hypoxic tumor regions.

Tumor hypoxia may profoundly lower choline metabolic trapping in cancer cells. Thus, choline tracer retention may be related to tumor oxygenation status through effects on choline kinase activity. This effect has clear implications for interpretation of clinical PET images with choline radiotracers; tumor proliferation (or viability) may be underestimated in hypoxic tumor regions.

CHAPTER II

Hypoxia downregulates expression of choline kinase α (ChKα) mediated by hypoxia inducible factor 1α (HIF1α)

1. Abstract

In this study, the effects of chronic hypoxia on ChKα expression were examined in PC-3 and LNCaP prostate cancer cells. RT-PCR analysis showed decreased transcription of ChKα gene in hypoxic PC-3 correlating with decreased enzymatic activity of choline kinase in hypoxic cell extracts. Over-expression of HIF1α in normoxic PC-3 cells decreased choline kinase mediated choline retention. Alignment of nucleotide sequence of the putative promoter region of ChKα from rat, mouse, chimpanzee and human revealed a highly conserved hypoxia responsive element, HRE7. Electrophoretic mobility shift competition/supershift assay and chromatin immunoprecipitation (ChIP) assay confirmed binding of HIF1 to HRE7. To understand the transcription control of ChKα under hypoxia, a putative promoter of ChKα was isolated from PC-3 genomic DNA and cloned into a luciferase (Luc) based reporter vector system. In PC-3, hypoxia decreased the expression of Luc under the control of the ChKα promoter. Mutation of HRE7 and subsequent Luc reporter assays demonstrated that this HRE is involved in hypoxia/HIF1-mediated regulation of ChKα. The results suggest that the decreased choline phosphorylation in PC-3 cells in response to hypoxia is mediated in part by transcriptional control of ChKα expression via HIF1 binding to HRE7.

2. Introduction

Tumors in general are heterogeneous in nature with regions of hypoxia and normoxia that are expected to have different metabolic profile. My work with different cancer cell lines discussed in the previous chapter, showed significant inhibition of choline phosphorylation in hypoxic condition (1% O_2) as compared to normoxic (21% O_2) cells. Inhibition of choline phosphorylation by hypoxia has not been reported as a universal response in cancer cell line and my previous observation provides a unique opportunity to understand the mechanism behind decreased choline metabolism in hypoxic cancer cells. Recently, increased choline kinase expression was reported by western blot in PC-3 cells exposed to 24 h hypoxia (1% O_2) (Glunde et al., 2008). $CoCl_2$ is known to stabilize HIF-1 protein (Groenman et al., 2007) as seen in hypoxia and is used to induce chemical hypoxia. HIF-1 activation of HREs within the putative ChKα promoter region was suggested to increase choline kinase expression under hypoxia or exposure to $CoCl_2$. The above mentioned report of increased expression of choline kinase in hypoxia contradicts my results on uptake of choline in hypoxia and recent microarray studies with PC-3 cells and MCF-7 breast cancer cells that showed ChKα to be significantly down-regulated by chronic hypoxia (Ackerstaff et al., 2007; Elvidge et al., 2006).

Although ChKα was shown to be up-regulated in hypoxia using promoter analysis, non-overlapping regions were identified in the ChKα promoter that can potentially up-regulate (HRE 3-6) or down-regulate ChKα (in red box) under chronic hypoxia, suggesting complex regulation of ChKα (Figure 17).

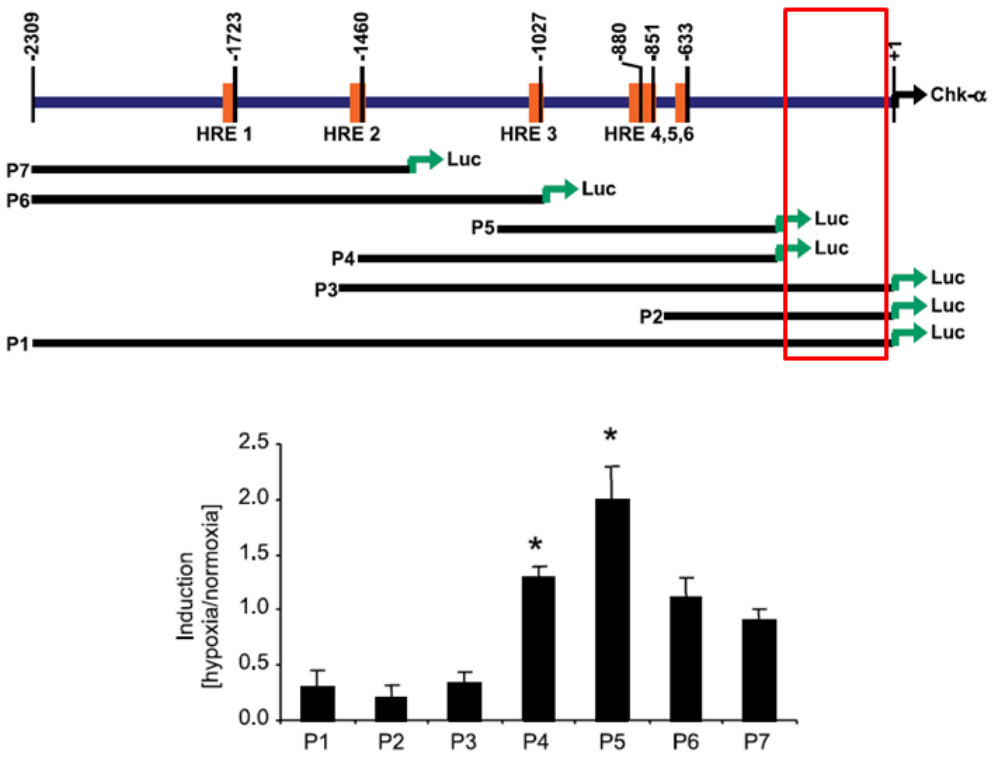

Figure 17. Schematic diagram of upstream promoter of human ChKα: Promoter region (in red box) is responsible for negative regulation of ChKα in hypoxia. Modified from Glunde et al., 2008.

The goals of the present study were to 1) evaluate the equilibrium status of the choline phosphorylation reaction in PC-3 cells to theoretically predict the effect of choline kinase inhibition on choline phosphorylation in these cells, 2) quantify ChKα mRNA expression and choline kinase activity in hypoxic PC-3 cells, 3) determine whether modulation of choline uptake and choline kinase activity is a HIF1α dependent response in PC-3 cells and 4) characterize the ChKα promoter associated with HIF1α mediated regulation of ChKα expression.

This study clarified that expression of ChKα is reduced in hypoxic PC-3 cells and identified a novel HIF1 binding HRE site that mediates down-regulation of ChKα in hypoxic PC-3 cells.

3. Materials and Methods

3.1. Material chart

Dr. Bunn HF, (Hematology Divison, Brigham & Women's Hospital, Boston, MA).	HIF1α/ pcDNA3 plasmid HIF1α(ΔODD)/ pcDNA3 plasmid
ATCC, Manassas, VA	PC-3 and LNCaP prostate cancer cells RPMI-1640 medium Fetal bovine serum 0.25% Trypsin-EDTA
Bio-rad, Hercules, CA	Bio-Rad protein assay reagent SDS Mini-Trans Blot system Mini-Protean electrophoresis system TBE polyacrylamide gel
Eppendorf, Westbury, NY	Centrifuge 5415R
Roche, Indianapolis, IN	Complete Protease Inhibitor Cocktail Tablets
Integrated DNA technology Inc., Coralville, IA	Oligonucleotide primers
Invitrogen, Carlsbad, CA	Oligofectamine LTX Quant-IT Picogreen quantification kit
Promega, Madison, WI	pGL4.74[hRluc/TK] pGL4.10 [luc2] Dual-Glo® Luciferase Assay System
New England BioLabs, Ipswich, MA	Phusion High-Fidelity PCR Master Mix with GC Buffer T_4 DNA ligase Restriction enzymes
Stratagene, La Jolla, CA	QuikChange Site-Directed Mutagenesis Kit
QIAGEN, Valencia, CA	RNeasy Plus mini Kit DNeasy Blood & Tissue Kit QIAquick PCR purification Kit minElute PCR purification Kit QuantiTect SYBR Green PCR Kit Q-solution gDNA Eliminator column

Perkin Elmer, Waltham, MA	Victor 3 Multiplate reader
GE Healthcare, Piscataway, NJ	Amersham Hyperfilm ECL
Santa Cruz Biotechnology, Santa Cruz, CA	anti-β-actin Anti-goat IgG HRP conjugate
Sigma, St. Louis, MO	Neomycin RIPA lysis buffer protease inhibitor cocktail
Novus Biologicals, Littleton, CO	polyclonal anti-HIF1□
Piercenet, Rockford, IL	LightShift Chemiluminescent EMSA Kit Chemiluminescent Nucleic acid Detection Module Biodyne B Nylon membrane
Eurofins MWG Operon, Huntsville, AL	PAGE purified biotinylated or unbiotinylated oligonucleotides
BD Biosciences, San Jose, CA	monoclonal anti-HIF1α
Applied Biosystems, Foster City, CA	TaqMan gene expression assays

3.2. Isolation of total RNA from cancer cells

RNA was isolated from 3 X 10^6 cancer cells using RNAeasy Mini Kit (QIAGEN Inc., Valencia, CA). The lysate was homogenized using QIAshredder spin column (QIAGEN Inc., Valencia, CA) according to manufacturer's instruction. Total DNA was separated from RNA using gDNA Eliminator column. The concentrations of total RNA were determined by absorbance at 260 nm with a Nanodrop spectrophotometer (Thermo Scientific, Wilmington, DE).

3.3. Quantification of mRNA signal

Expression of mRNA for ChKα was measured in the two cancer cell lines in normoxic and hypoxic conditions by real-time PCR using TaqMan® Gene

Expression Assays on ABI PRISM 7700 Sequence Detection System (Applied Biosystems, Foster City, CA). ~ 5 µg of total RNA of each sample was used to generate cDNA and the real-time PCR reactions were carried out following the manufacturer's protocol. 18S rRNA was used as an endogenous control.

3.4. Western blot analysis

Cells were homogenized with radioimmunoprecipitation assay (RIPA) lysis buffer (SIGMA) containing protease inhibitor cocktail. Cell extracts were obtained by centrifugation for 10 min at 4°C and 8000 x g. Protein concentrations were determined by the Bio-Rad assay. Equal amounts of protein were separated on SDS-polyacrylamide gels; fifty µg of protein was separated for HIF1α and β-actin. At the end of separation, the proteins were transferred to a PVDF (polyvinylidene difluoride) membrane by the wet blotting method, and probed with antibodies directed against hypoxia inducible factor 1α (HIF1α) and β-actin. The amounts of bound antibodies were accessed by the peroxidase activity of horseradish peroxidase-conjugated secondary antibody as detected by Amersham ECL Plus Western Blotting Detection Reagents.

3.5. Over-expression of hypoxia inducible factor 1α (HIF1α)

Full length HIF1α and HIF1α (ΔODD) expression constructs expressing respective proteins (Figure 18) were kindly provided by Dr. H Franklin Bunn (Hematology Divison, Brigham & Women's Hospital). Stable PC-3 cell lines expressing HIF1α were generated following transfection with Lipofectamine LTX reagent (Invitrogen, Carlsbad, CA, USA) and neomycin selection (200 µg/ml).

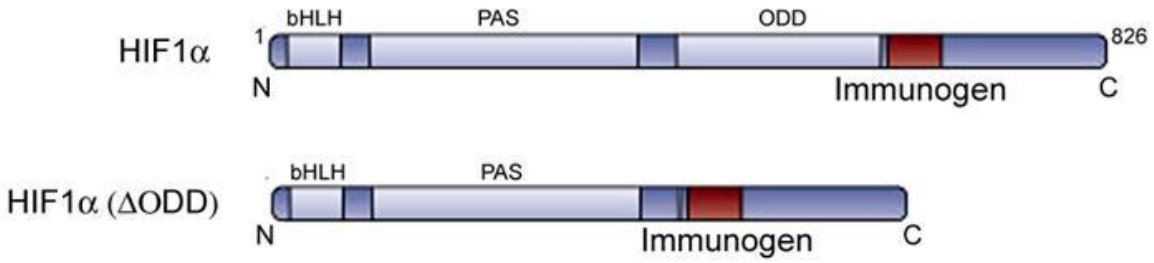

Figure 18. Schematic diagram of HIF1α inserts in the expression vector. These inserts were used in the expression vector for expressing HIF1α protein and oxygen stable HIF1α (ΔODD) protein without oxygen dependent degradation domain.

3.6. Isolation of promoter region upstream of choline kinase α (ChKα)

The genomic DNA was extracted from PC-3 using DNeasy Blood & Tissue Kit (Qiagen) and quantified. Putative promoter region upstream of ChKα was amplified from genomic DNA using Phusion High-Fidelity PCR Master Mix with GC Buffer (NEB, Ipswich, MA, USA). The identity of the promoter was confirmed using nested PCR amplifications and sequencing. Details of primers used are described in Table 6. Amplified full length promoter had restriction sites, Acc651 and HindIII at the 5' and 3' end, respectively, for directed cloning into the pGL4.10 [luc2] vector (Promega, Madison, WI, USA).

3.7. Promoter alignment

To identify conserved putative HIF1α binding site alignment of promoter region upstream of rat, mouse, chimp and human choline kinase α was done using online Clustal W program, http://www.ebi.ac.uk/Tools/clustalw2/index.html.

Table 6. Sequences of primers used for ChKα promoter isolation and nested PCRs.

Region	Primer	Amplicon size (bp)
Full length promoter	Forward primer 5'-GCGGGTACCTGAGGCAACCTCTTCCTCC-3' Reverse primer 5'-GCGAAGCTTTGCCCGACAGGCGGCCGA-3'	2190
Nested PCR 1	Forward primer 5'-GCGGGTACCTGAGGCAACCTCTTCCTCC-3' Reverse primer 5'-GACCGTGACTAACGCACCTT-3'	1091
Nested PCR 2	Forward primer 5'-TGGAAGACTGTGAACTCCCC-3' Reverse primer 5'-GCTCAGTGGGTGTGATTTT-3'	658
Nested PCR 3	Forward primer 5'-AAGGTGCGTTAGTCACGGTC-3' Reverse primer 5'-GCGAGAGGACTAGGCTCAGA-3'	1081
Nested PCR 4	Forward primer 5'-GAGGGGTCCAAGGAAACTTT-3' Reverse primer 5'-GCGAAGCTTTGCCCGACAGGCGGCCGA-3'	584

3.8. Site-directed mutagenesis

Mutation at the conserved putative HIF1α binding site (5'-TCGTGC-3') to (5'-AGCATT-3') was performed using QuikChange Site-Directed Mutagenesis Kit (Stratagene, La Jolla, CA, USA).

3.9. DNA sequencing

DNA sequences of all plasmids were confirmed by sequencing by DNA Core Sequencing Facility at Brigham and Women's Hospital, Boston, MA.

3.10. Transient expression assays

PC-3 cells were cultured in RPMI-1640 medium containing 10% fetal bovine serum (FBS) on 100 mm dishes at 37°C with 5% CO_2 in air. When cell confluence reached about 80%, the media were removed and the cells were washed with 1X phosphate buffered saline (PBS). The cells were detached with 1X Trypsin-EDTA (0.25% Trypsin, 1 mM EDTA). After detaching, one third of the cells were transferred to fresh RPMI-1640 medium containing 10% FBS on 100 mm dishes and incubated at 37°C with 5% CO_2. For transient expression, PC-3 cells were inoculated into 6 well plates and incubated overnight in RPMI-1640 medium containing 10% FBS at 37°C with 5% CO_2. Following overnight incubation, the media were changed to OPTI-MEM reduced serum medium. The firefly luciferase reporter plasmid, pGL4.10 [luc2] containing the human ChKα promoter region and pGL4.74[hRluc/TK], the internal control plasmid expressing renilla luciferase, were cotransfected using Lipofectamine LTX following the instructions of the manufacturer. Following 24h of normoxia (21% O_2) or hypoxia (1% O_2), transfected cells were lysed and expression assays were performed using Dual-Glo® Luciferase Assay System (Promega).

3.11. Electrophoretic Mobility Shift Assay (EMSA)

Nuclear proteins were prepared using the NE-PER nuclear and cytoplasmic extraction kit (Piercenet, Rockford, IL, USA). Complementary PAGE purified biotinylated or unbiotinylated oligonucleotides (Eurofins MWG Operon, Huntsville, AL, USA) were annealed to make double-stranded probes. Details of the probes are described below (Table 7). The labeled probes were incubated with hypoxic PC-3 cell nuclear extracts according to manufacturer's protocol in LightShift Chemiluminescent EMSA Kit (Piercenet). The DNA-protein complexes was resolved in 5% nondenaturing TBE polyacrylamide gel (Biorad, Hercules, CA), followed by wet transfer to Biodyne B Nylon membrane (Piercenet). Complex was detected using Chemiluminescent Nucleic acid Detection Module (Piercenet). For competition assays, 4 pmol (200 times excess) unlabeled probes and 0.5 µg monoclonal anti-HIF1α (BD Biosciences) was used. For supershift assay, 0.5 µg polyclonal anti-HIF1α (Novus Biologicals, Littleton, CO) was used. Incubation without nuclear extract was used as a negative control.

Table 7. Sequence of double stranded (ds) probe used for electrophoretic mobility shift assays.

Probe	Sequence of first strand of the ds probe	Reference
Labeled HRE7	Biotin-5'-GCGGCCGGCGCTCCTCGTGCGGCGGCGGCAGAGG-3'	Present work
Unlabeled HRE7	5'-GCGGCCGGCGCTCCTCGTGCGGCGGCGGCAGAGG-3'	Present work
Unlabeled HRE upstream VEGF	5'-TGCATACGTGGGCTCCAACAG-3'	(Nguyen and Claycomb, 1999)

3.12. Chromatin immunoprecipitation (ChIP) assay

The assay was performed based on standard ChIP assay protocol (Xia and Kung, 2009; Xia et al., 2009). Chromatin was sonicated to 500- to 1,000-bp fragments and immunoprecipitation was carried out with polyclonal anti-HIF1□ (Novus Biologicals). Chromatin (sonicated or immunoprecipitated) were purified by standard phenol-chloroform procedure followed by column purification using minElute PCR purification kit (Qiagen). DNA was quantified by Quant-IT Picogreen quantification kit (Invitrogen, USA). Equal amount of unprocessed (Input) and immunoprecipitated (ChIP) chromatin was used for PCR. Traditional PCR was performed to standardize conditions for quantitative PCR. Q-solution (Qiagen) additive was included in amplification of promoter region spanning the HRE7 site due to high GC content of the amplicon. Fold enrichment of a

promoter region was assessed by performing quantitative PCR using QuantiTect SYBR Green PCR Kit (Qiagen) with chromatin samples taken before (input) and after immunoprecipitation (ChIP). Details of the primers and calculations for fold enrichment are described below (Table 8).

Table 8. Sequences of primers used for PCR for amplification of promoter regions in ChIP assay.

Promoter region	Forward primer	Amplicon size (bp)	Reference
Negative control region (10kb upstream of VEGF)	Forward primer 5'-TTGATGTAGGCAGAACCTGGGAGA-3' Reverse primer 5'-CCCGCCCAGAAAGGTTTGTTAAGT-3'	159	(Xia and Kung, 2009; Xia et al., 2009)
Positive control region (HRE upstream ENO1)	Forward primer 5'-AGATAGGACCGGTGAGCCGAACT-3' Reverse primer 5'-AAAGTTGTCAGCAAGGTCGAGGG-3'	171	(Xia and Kung, 2009; Xia et al., 2009)
HRE7	Forward primer 5'-AATCAGTGGCGAGCGCGAGG-3' Reverse primer 5'-TGGAGCGGGGATGTGCTGCT-3'	102	Present work

3.13. Statistical analysis

Results are presented as means ± standard deviation. Student's t-test was applied for statistical evaluation and a p-value <0.05 was considered significant.

4. Results

4.1. Hypoxia decreases the expression of choline kinase α (ChKα) in prostate cancer cells

Hypoxic exposure to PC-3 cells was able to significantly elevate the expression of HIF1α protein as shown by western blot analysis (Figure 19). Existence of a HIF1α dependent response in hypoxic PC-3 was confirmed with RT-PCR, showing significantly increased mRNA levels of VEGF gene (2.5 fold) under chronic hypoxia (Table 9). Supporting the decreased choline kinase activity, RT-PCR analysis showed significant decrease in mRNA levels of ChKα gene in PC-3 cells. Similar effect of hypoxia on HIF1α, VEGF and ChKα expression was seen in another prostate cancer cell line, LNCaP (Table 9).

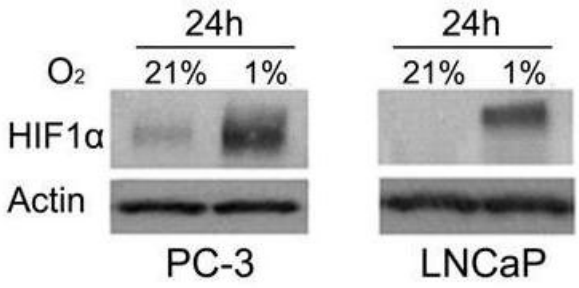

Figure 19. **Effect of hypoxia on expression of HIF1α** HIF1α protein levels shown by western blot

Table 9 Effect of 24h of hypoxic (1% O_2) exposure on expression of ChKα and VEGF mRNA

	mRNA level ratio (Hypoxia/Normoxia)	
	ChKα	**VEGF (+ control)**
PC-3	0.74 ± 0.12	2.44 ± 0.4
LNCaP	0.71 ± 0.13	5.05 ± 0.81

Values less than 1 means down-regulation and values more than 1 means up-regulation of mRNA expression in hypoxia

4.2. Over-expression of HIF1α decreases uptake and phosphorylation of choline in prostate cancer cells

Hypoxia decreased choline kinase activity and choline uptake in PC-3 cells but it was not clear that this reduction was mediated by HIF1α. Stable cell lines over-expressing full length HIF1α (negative control) and HIF1α lacking oxygen dependent degradation domain (ODD) were successfully generated. The expression status of these cell lines were confirmed by western blot with monoclonal antibody against HIF1α (Figure 20a). Deletion of ODD in HIF1α protein was able to prevent degradation of this protein in normoxic condition. Choline uptake (Figure 20b) and choline activity (Figure 20c) were both decreased in normoxic PC-3 cells that were over-expressing stabilized HIF1α, thus mimicking the effects of hypoxia.

4.3. HIF1 binding sites and promoter alignment

HIF1 regulates gene expression by binding to hypoxia response core element(s) (HRE, 5'- CGTG - 3') in the proximal promoter region of the hypoxia responsive genes (Semenza et al., 1998). In the promoter region upstream of

human choline kinase α (hChKα), 6 previously identified HRE sites relative to +1 translation start site (Glunde et al., 2008) were confirmed as HRE1 (-1723); HRE2 (-1460); HRE3 (-1027); HRE4 (-880); HRE5 (-851); and HRE6 (-825) (Figure 21). In addition to these, two putative HRE sites were newly identified as HRE2B (-1422) and HRE7 (-222). DNA sequence alignment of promoter region upstream of the hChKα (Glunde et al., 2008), chimp (from NCBI), rat (Uchida et al., 1994) and mouse (from NCBI) showed that out of these 8 putative HRE sites in the proximal promoter region only HRE7 positioned at -222 nucleotide was conserved across all species (Figure 21).

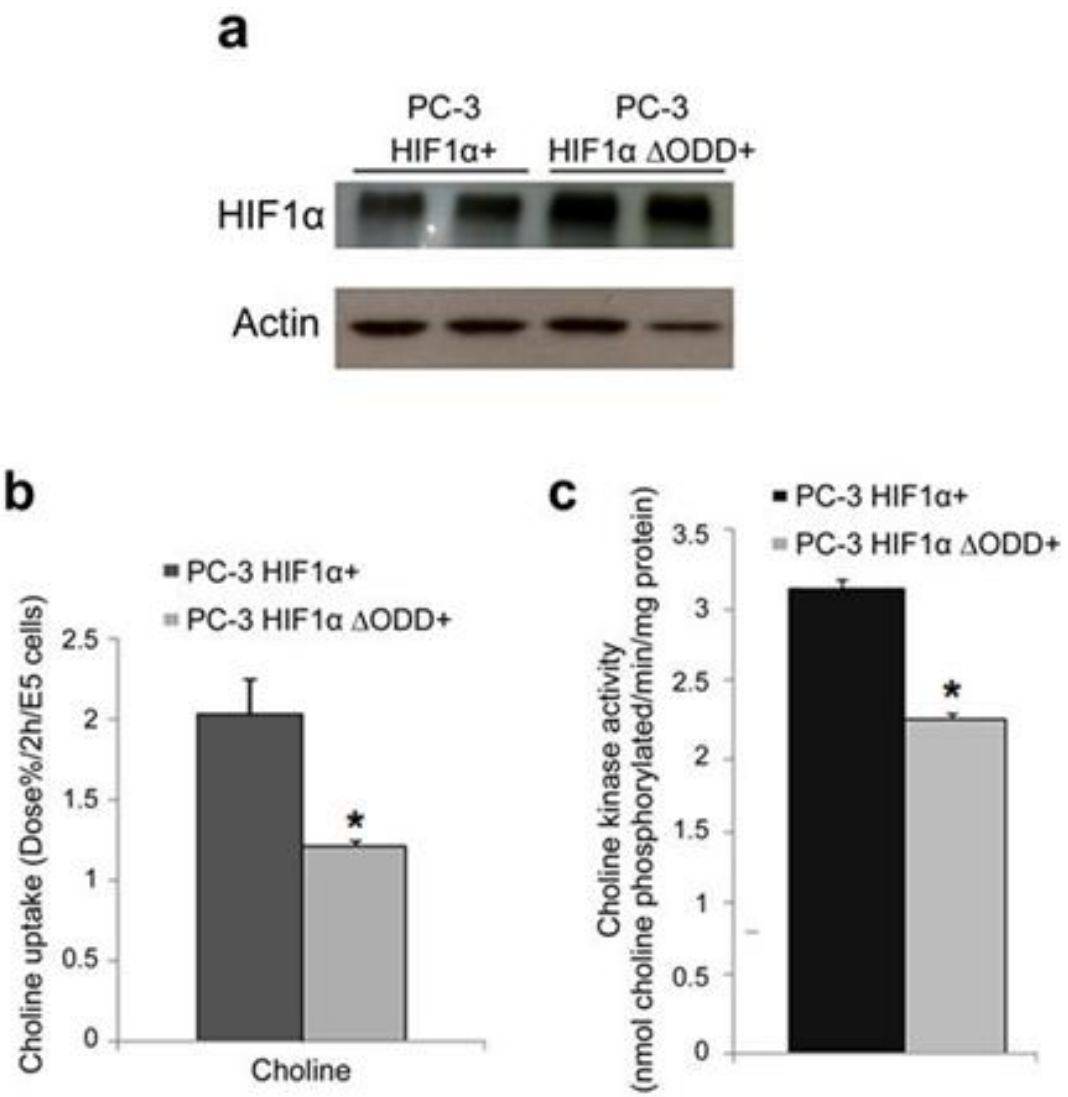

Figure 20. Effect of HIF1α on choline metabolism. (a) Over-expression of full length HIF1α and HIF1αΔODD+ in PC-3 cells as shown by western blot on (b) choline tracer uptake (n = 3, each condition) and (c) choline kinase activity (n = 3, each condition). The cells expressing variant of HIF1α lacking the oxygen dependent degradation domain (ODD) showed significantly ($p < 0.05$) reduced [^{3}H]choline uptake and choline kinase activity. * $p < 0.05$ Vs values in PC-3 HIF1α+ control using unpaired t-test.

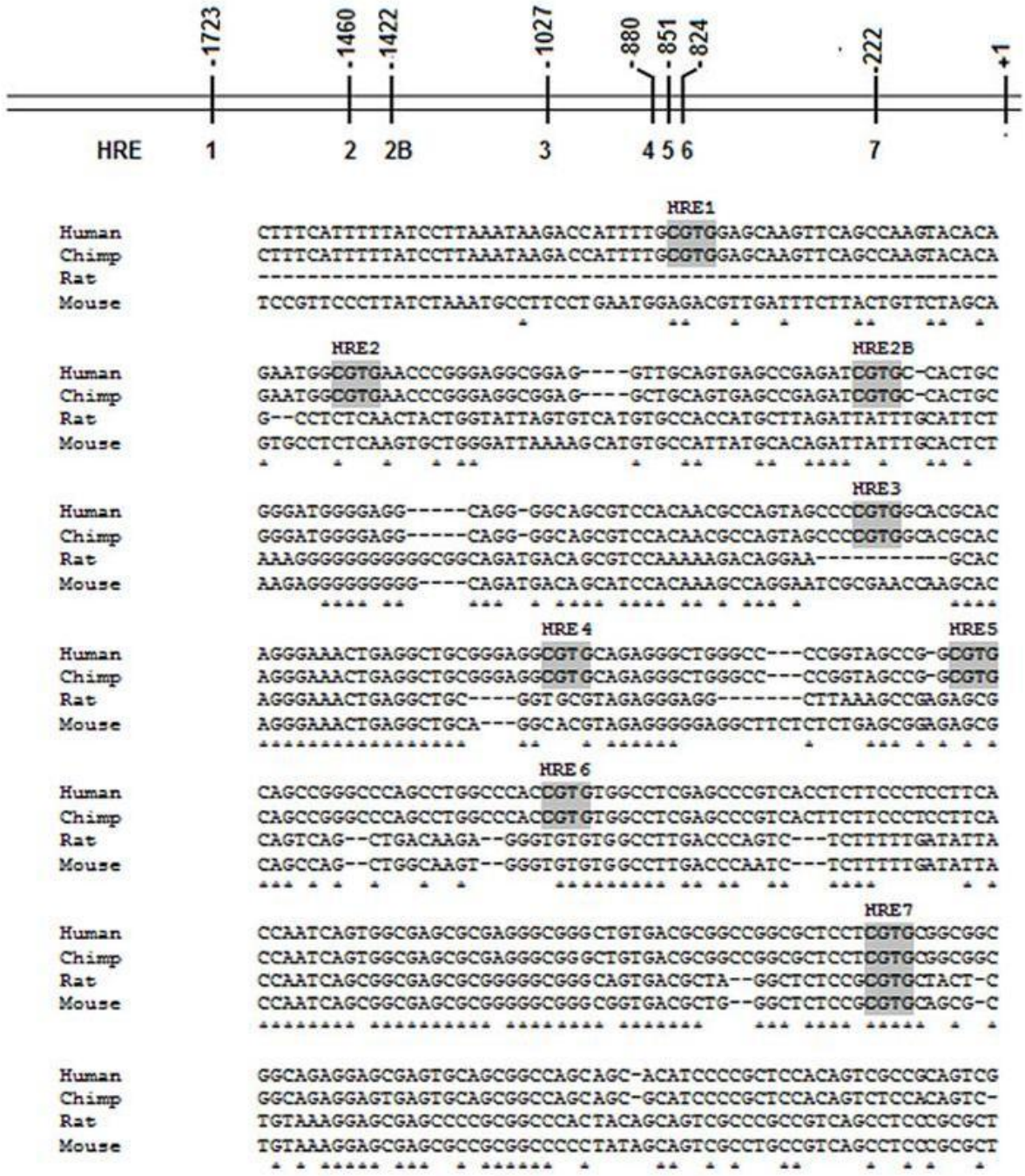

Figure 21. Nucleotide alignments of segments of promoter region upstream of ChKα gene: Alignment of human, chimp, rat and mouse showing 8 putative HRE sites in the promoter region of ChKα promoter. The schematic diagram and HRE nomenclature was adapted from Glunde et al., (2008).

4.4. Mutation of a putative HRE site reduced the inhibitory effect of HIF1α on ChKα promoter activity in PC-3 prostate cancer cells

The proximal promoter (~ 2.2 Kb) upstream of hChKα was successfully isolated from PC-3 genomic DNA and cloned into luciferase vector construct. This was confirmed with nucleotide sequencing and amplification with nested primers. Mutation at the conserved HRE7 site (5'-TCGTGC-3') to (5'-AGCATT-3') in the promoter of the construct was successful and confirmed by nucleotide sequencing. In normoxic conditions, there was no difference in promoter mediated luciferase signal from PC-3 cell lines expressing wild type HRE7 and mutated HRE7 (Figure 22). In contrast, in hypoxic and DMOG treated PC-3 cells, there was a significant decrease in luciferase signal from PC-3 cells expressing wild type HRE7 as compared to normoxic cells and cells with no DMOG exposure. However, in hypoxic or DMOG treated cells expressing mutated HRE7, there was a slight increase in luciferase signal when compared to normoxic levels or cells expressing wild type HRE7 (Figure 23).

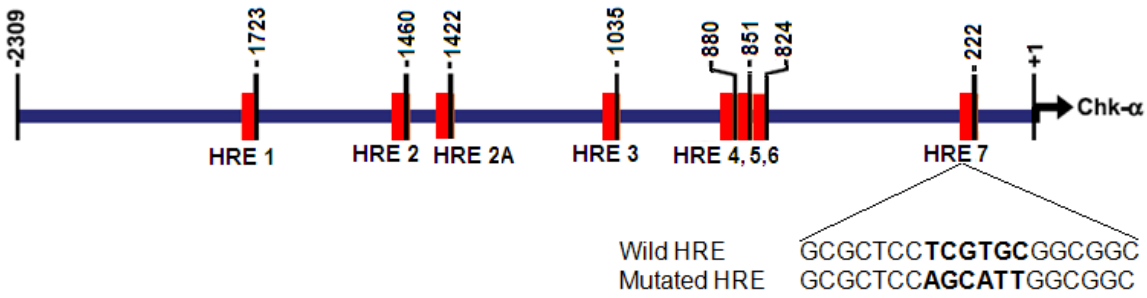

Figure 22. Schematic diagram of human ChKα promoter showing the site and description of mutation. HRE nomenclature was adapted from Glunde et al., 2008.

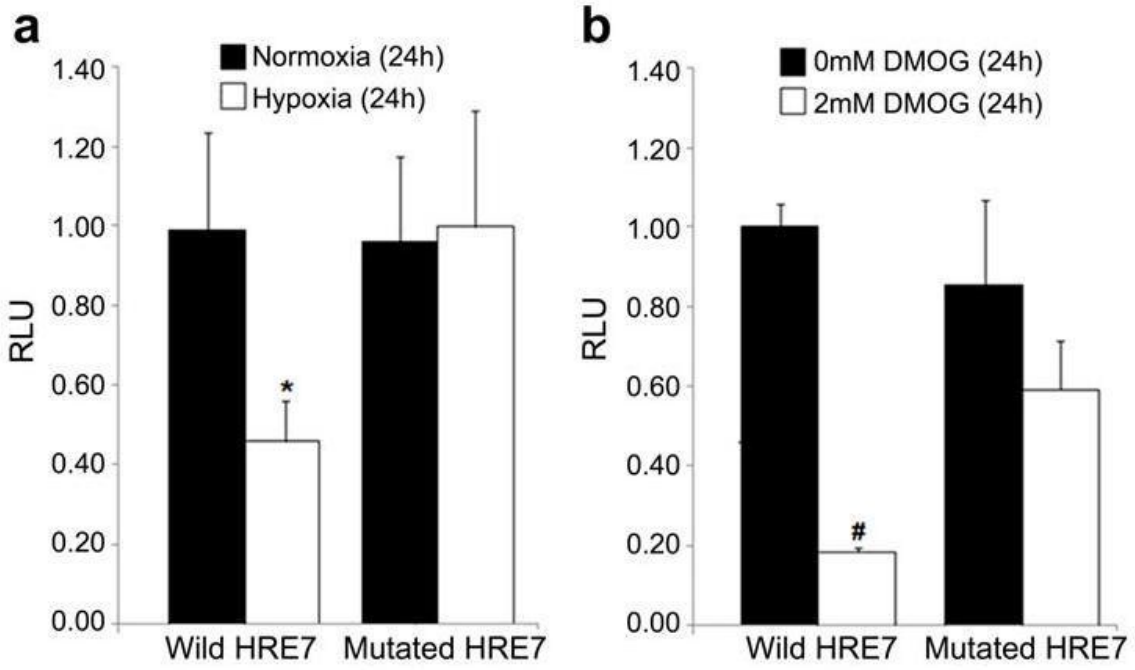

Figure 23. Promoter - reporter construct assay: Wild type and mutated ChKα gene promoter dependent luciferase signal from PC-3 cells expressing wild type promoter and mutated promoter in (a) normoxia (21% O_2) and hypoxia (0% O_2), and in (b) presence of 0 mM DMOG and 2 mM DMOG. Hypoxia (*$p < 0.05$ Vs normoxia) and DMOG ($^{\#}p < 0.1$ Vs 0mM DMOG) reduced luciferase signal with wild type ChKα promoter but had no significant effect with the mutated HRE7.

4.5. HIF1α is able to bind to the putative HRE site in ChKα promoter

An electrophoretic mobility shift assay (EMSA) was performed to assess the binding ability of HIF1 to HRE7 in *in vitro* conditions (Figure 24). Lane 1 and 5 showed only a single band of unbound or free biotinylated probe (containing HRE7 site). With the addition of the nuclear protein extract of hypoxic PC-3 cells in the binding reaction, an extra band of decreased mobility was observed (Figure 24; Lane 2 and 6). This extra band represented binary complex HIF1-biotinylated probe complex. The binary complex was not visible when the binding assay was performed with unlabeled probe (with HRE7 site) added 200 times in

excess of the biotinylated probe (Figure 24; Lane 3), demonstrating saturability of binding. A significant decrease in intensity of the extra band was also seen when unlabeled probe with known functional HRE site upstream of HIF1 regulated VEGF gene was added in 200 times in excess of the biotinylated probe (Figure 24; Lane 4). Incubation with specific monoclonal antibody against HIF1 prevented binding of HIF1 to biotinylated probe (Figure 24; Lane 7). Specific polyclonal antibody against HIF1α did not disrupt the HIF1-biotinylated probe complex but formed a tertiary complex of anti-HIF1α, HIF1, and biotinylated probe. This tertiary complex was seen as an extra band on acrylamide gel that was above the band represented by the HIF1α-biotinylated oligo binary complex (Figure 24; Lane 8). This supershift of biotinylated probe was caused due to significant decrease in mobility of the tertiary complex.

A ChIP assay was performed to determine whether HIF1 binds to the putative HRE 7 site in vivo in normoxic and hypoxic PC-3 cells. Hypoxia was mimicked by incubation with 2 mM DMOG. Using traditional PCR, we could observe significant enrichment of promoter regions with HRE7 (Figure 25a) after immunoprecipitation as compared to input samples in hypoxia. The enrichment in hypoxia and normoxia was quantified from threshold Ct values obtained by quantitative PCR (Figure 25b). Based on quantitative PCR results, following ChIP, HRE7 showed 7.7-fold enrichment in hypoxia as compared to 2.3- fold enrichment in normoxia, suggesting increased binding of HIF1 to HRE7 in hypoxic conditions.

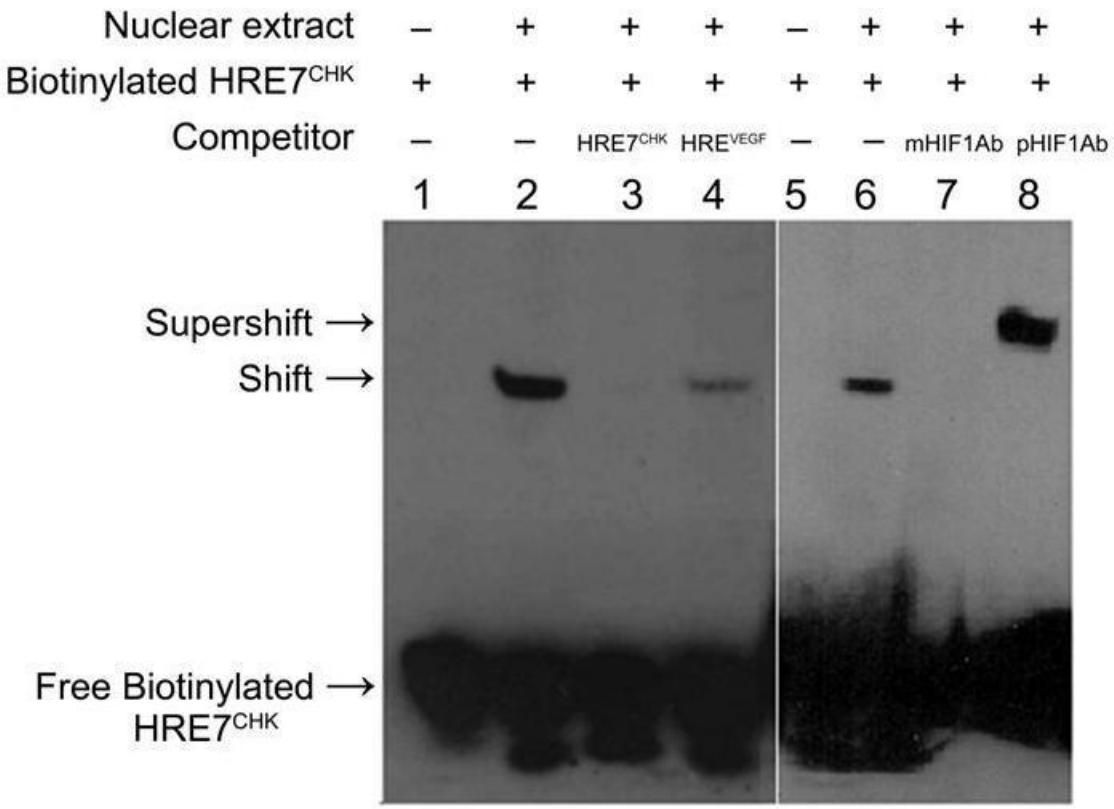

Figure 24. In vitro binding of HIF1 to HRE 7 site of human ChKα promoter. Electrophoretic mobility shift competition and supershift assay using nuclear extract from hypoxic PC-3 cells. $HRE7^{CHK}$ - 200 fold excess of unlabeled probe with HRE7 site; HRE^{VEGF} - 200 fold excess of unlabeled probe with functional HRE upstream of VEGF; mHIF1Ab - monoclonal anti - HIF1α and pHIF1Ab- polyclonal anti-HIF1α.

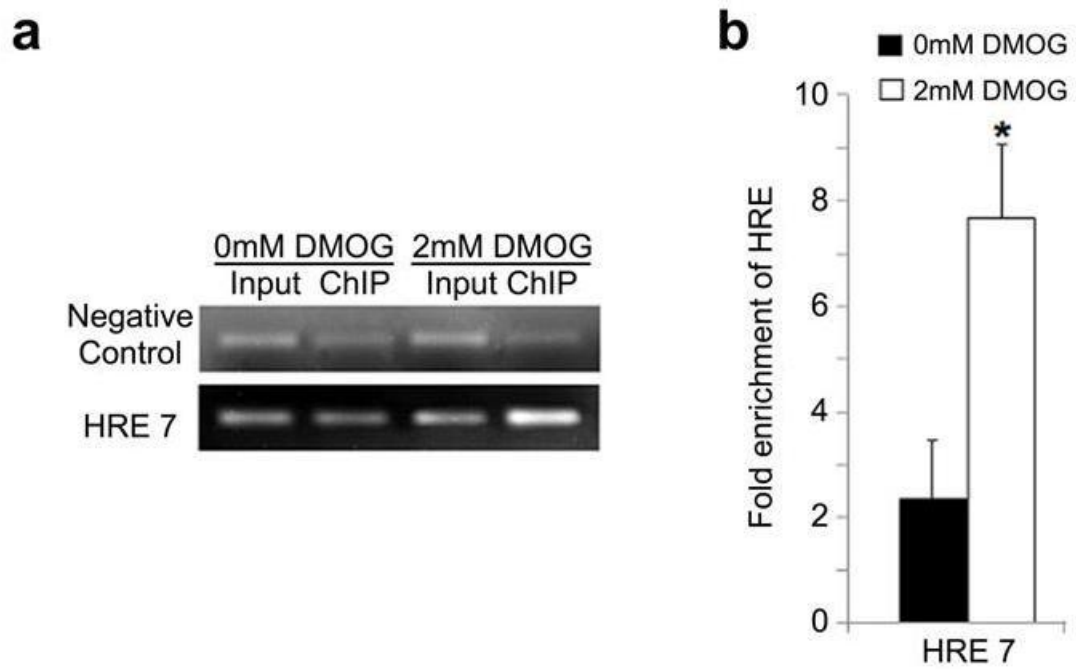

Figure 25. In vivo binding of HIF1 to HRE 7 of hChKα promoter region in PC-3 cells by ChIP assay. Following 24h exposure to normoxia (0 mM DMOG) or hypoxia (2 mM DMOG), chromatin was cross-linked, sonicated and immunoprecipitated with polyclonal anti-HIF1α. PCR was performed with reverse-crosslinked chromatin samples taken before (input) and after immunoprecipitation (ChIP). Enrichment of chromatin fragment including the specific HRE in immunoprecipitated chromatin was compared to unprocessed chromatin (input) by (a) representative gel of semi-quantitative PCR and gel electrophoresis and (b) quantitative PCR (n = 5, each condition). Fold enrichment calculated by quantitative PCR was normalized with negative control. Negative control used was a region upstream of VEGF gene that contained no HRE site. DMOG caused a significant fold increase in enrichment of HRE7. * $p < 0.05$ Vs values in 0mM DMOG (control) using unpaired t-test.

5. Discussion

We are the first to report a decreased expression of ChKα in hypoxic PC-3 and LNCaP prostate cancer cells using RT-PCR. Similar findings with microarray analysis were reported in hypoxic PC-3 and MCF-7cells (Elvidge et al., 2006; Ackerstaff et al., 2007). The decreased mRNA levels correlated with decreases in choline kinase activity in protein extracts of hypoxic PC-3 cells. These results

suggest hypoxia-induced transcriptional control of the ChKα gene. In MCF-7, siRNA HIF1α silencing has been previously reported to abolish the negative effect of hypoxia on ChKα expression (Elvidge et al., 2006; Ackerstaff et al., 2007). In the present study, we have shown that over-expression of HIF1α in normoxic PC-3 cells is sufficient to decrease choline uptake and choline kinase activity independent of hypoxia. Thus, there is strong evidence of HIF1α mediated negative control of choline phosphorylation in cancer cells.

Transcriptional control of hypoxia responsive genes by HIF1α is mediated by binding of HIF1α to HRE sites in the regulatory promoter region of a target gene (Caro, 2001). In our analysis of the promoter region of the hChKα we confirmed the 6 HRE sites previously reported with the sequence 5'-G/CCGTG-3' (Glunde et al., 2008). In our study we included two additional potential HIF1α binding sites with sequence 5'-TCGTG-3' (HRE2B and HRE7) following a previous report on the ability of 5'-TCGTG-3' to bind to HIF1α in promoter region of hypoxia responsive phosphoglycerate kinase -1 (PGK-1) (Okino et al., 1998). Hypoxia-induced inhibition of choline phosphorylation and choline kinase activity has been reported in cancer cell lines derived from mouse (Sarri et al., 2006) and humans (Hara et al., 2006). Alignment of nucleotide sequence of promoter of ChKα gene from rat, mouse, chimp and human was performed in order to find conserved putative HRE sites that could potentially be mediating a universal hypoxic response. Alignment of promoters revealed that not all putative HRE core sites are conserved across species. We found only one well conserved HRE site, HRE7 at the -222 nucleotide position.

Binding of HIF1 to HRE7 was confirmed by electrophoretic mobility shift assay (EMSA). Furthermore, the HRE from the promoter region of VEGF (Nguyen and Claycomb, 1999) gene was able to compete with the HRE7 of ChKα for HIF1 binding in nuclear extracts derived from hypoxic PC-3 cells. It was interesting to note that HIF1 showed a higher binding affinity for HRE7 than for the HRE upstream of VEGF gene. Specific monoclonal antibody against HIF1α inhibited binding of HIF1 to HRE7. In addition, a polyclonal antibody against HIF1α was able to form a tertiary complex with HRE7-HIF1 causing supershift on the acrylamide gel. These results strongly support *in vitro* binding of HIF1 to HRE7. The *in vivo* binding of HIF1 to the conserved HRE7 was confirmed by ChIP assay. Following DMOG exposure, significant enrichment of chromatin fragments with HRE7 was found, indicating HRE7 is sensitive to changes in HIF1 levels.

Observations in the present study are in well accordance with previously reported microarray and choline tracer studies with hypoxic PC-3 cells and MCF-7 cells (Ackerstaff et al., 2007; Elvidge et al., 2006; Hara et al., 2006). In addition, the present study also corroborate the work of Glunde et al.,2008 that suggested involvement of HRE 3-6 in hypoxia mediated potential up-regulation of ChKα expression. It should be noted that in their study, HRE 3-6 exerted a positive effect on expression of the reporter in hypoxia only when the highly repressive downstream +1 to -338 nucleotides was deleted from the promoter constructs. Based on the present work we have shown that this highly repressive downstream ~ 338bp ChKα promoter region contains the conserved HIF1

binding HRE7 site. The role of HRE7 in transcriptional down-regulation of ChKα was confirmed when the mutation of HRE7 abrogated the transcriptional repressive control of full length ChKα promoter under hypoxia or DMOG exposure in the promoter-luciferase construct assays.

From a survey of the literature on various genes, HIF1α is reported to exclusively up-regulate (Semenza et al., 1994; Firth et al., 1995; Semenza et al., 1996; Riddle et al., 2000; Chen et al., 2001) or down-regulate (Eltzschig et al., 2005; Rosenberger et al., 2007; Zheng et al., 2009) its target gene. The presence of multiple HIF1 binding HRE sites (HRE 3-6 and HRE7) in the ChKα promoter region with opposing effects on expression of ChKα in hypoxia appears to be unique. Thus the regulatory mechanisms whereby HIF1 influences ChKα expression are complex and deserve further study.

It is tempting to speculate that HIF1 mediated transcriptional down-regulation of ChKα gene could represent a survival strategy for hypoxic cancer cells. Choline phosphorylation is ATP consuming. Thus, a reduction in choline kinase activity may have an ATP sparing effect in energy starved hypoxic conditions. Cancer cells must survive hypoxic stress by prioritizing use of ATP in various ATP requiring processes in the cell. Additional work is needed to further understand the role and importance of HIF1 mediated inhibition of choline kinase expression/choline phosphorylation in hypoxic conditions. High Km for ATP for choline kinase makes it possible for choline kinase to be modulated by changes in ATP levels. Increased choline phosphorylation in cancer cells is the basis for choline-based imaging modalities for cancer diagnosis and therapy monitoring.

Tumors that are hypoxic may exhibit low accumulation of choline as governed by increased efflux of non-metabolized choline and decreased metabolic trapping (phosphorylation). Thus, interpretations of total choline signal from MRSI and clinical PET images with choline radiotracers should bear in mind that the hallmark up-regulations of choline-containing metabolites, choline uptake and choline phosphorylation may be significantly blunted in hypoxic tumor regions. Anticancer therapies that modulate tumor hypoxia (Yeo et al., 2004) may have secondary effects on choline kinase expression and activity. Therefore, the potential impact of changes in tumor oxygenation on the signals of choline-based imaging methods should be considered when imaging studies are used to noninvasively monitor treatment response in hypoxic tumors.

My present work provides strong evidence that choline phosphorylation step is far from equilibrium in human prostate cancer cell line, PC-3 and that hypoxia down-regulates ChKα expression. This regulation involves transcriptional level mediation by HIF1 at the conserved HRE7 site in ChKα promoter.

CHAPTER III

Choline kinase expression and hypoxia confers a survival advantage to early stage prostate cancer cells

1. Abstract

ChKα and hypoxia are associated with aggressive tumor phenotype. This study shows how prostate cancer cells, PC-3 (late stage and androgen-independent cell lines) and LNCaP (early stage and androgen-dependent cell lines), respond to over-expression of ChKα and chronic hypoxia (1% O_2) (independently and in combination). Over-expression of ChKα decreased cell proliferation rate and cell invasion potential of PC-3 cells irrespective of exposure to normoxia or hypoxia. On the other hand, in LNCaP cells, over-expression of ChKα and hypoxia independently increased proliferation rate and markedly increased cell invasiveness correlating with increased expression of pro-migratory factor, uPa. In both cell lines, over-expression of ChKα had a positive effect on anchorage independent growth which was more pronounced in LNCaP than in PC-3 but hypoxia inhibited the anchorage independent growth in both cell lines. In conclusion, differential effects were observed in PC-3 and LNCaP cells lines in response to ChKα over-expression and hypoxia. Greater enhancements of malignant phenotypes were observed in the more differentiated LNCaP cell line. The results suggests that increased ChKα activity and hypoxic tumor microenvironment are important for progression of early-stage, androgen-

dependent prostate cancer but confer little survival advantage in undifferentiated, androgen-independent prostate cancers.

Introduction

All human tumors encounter hypoxia during their development (Anastasiadis et al., 2002). It has been demonstrated that tumor hypoxia can be an independent prognostic indicator of poor clinical outcome in patients with head and neck cancers, cervical cancers, and soft tissue sarcomas (Anastasiadis et al., 2002). Hypoxia is common in primary prostate tumors too and is usually associated with poor prognosis (Movsas et al., 1999). Recent studies show that prostate cancer cells are able to survive tumor hypoxia (≤ 1% O_2). These surviving cancer cells develop aggressive malignant phenotypes and become resistant to androgen ablation, radio- and chemotherapy (Movsas et al., 2000).

To understand the survival adaptations in hypoxic prostate tumors, experimental model systems of prostate cancer, LNCaP and PC-3 can be useful. These two cell lines represent different stages of prostate cancer disease progression. LNCaP represents androgen-dependent, early stage cancer with a low invasion potential (Langeler et al., 1993) whereas PC-3 cells represents androgen-independent, late stage cancer with high invasion potential (Kaighn et al., 1979).

Our earlier work with LNCaP and PC-3 has shown that both cell lines are able to survive low oxygen environment for 48h (Hara et al., 2006). Although there was no loss in cell viability, the hypoxic cells showed significantly reduced cell proliferation rate as compared to their normoxic counterparts. Recently,

chronic hypoxia was reported to decrease invasion potential of highly aggressive PC-3 cells (Ackerstaff et al., 2007). As chronic hypoxia is well reported to facilitate cancer aggressiveness, it is important to assess the responses to chronic hypoxia in the context of disease progression stage of the cancer cells. This knowledge is useful in developing stage-specific cancer therapeutic strategies.

Development of aggressive malignant phenotype in hypoxia occurs by modulating various biochemical and physiological processes (Vaupel et al., 1989). Among the various biological processes modulated in hypoxia, we are interested in choline uptake and phosphorylation as it is often associated with high cell proliferation and tumor aggressiveness (DeGrado et al., 2001; Katz-Brull et al., 2002; Ramirez de Molina et al., 2002). Choline uptake and phosphorylation in tumors can be easily monitored by imaging techniques like PET (Shinoura et al., 1997; DeGrado et al., 2001) thereby allowing non-invasive cancer diagnosis. Interestingly, both choline uptake and phosphorylation is decreased in hypoxic prostate cancer cells. In PC-3 and LNCaP cells after 4h of hypoxia (0% O_2), PC-3 showed 15% decrease in choline uptake, whereas LNCaP showed 28% decrease in choline uptake (Hara et al., 2006). My work covered in previous chapters and recent work with hypoxic prostate cancer and breast cancer cell line, MCF-7 (Elvidge et al., 2006; Hara et al., 2006; Ackerstaff et al., 2007) has shown that the reason for reduced choline uptake and phosphorylation is in part due to down-regulation of expression of choline kinase in hypoxia. Down-regulation of choline phosphorylation could possibly represent a crucial survival

strategy for hypoxic cancer cells. Choline phosphorylation is ATP consuming. Cancer cells must survive hypoxic stress by prioritizing use of ATP in various ATP requiring processes in the cell (Vaupel et al., 1989). Thus, a reduction in choline kinase activity may have an ATP sparing effect in energy starved hypoxic cells. Although decreased choline phosphorylation may conserve energy, but its survival advantage of decrease choline kinase expression in terms of its effect on malignant phenotypes of hypoxic cancer cells is at present not known.

The goals of the present study were to 1) compare the effect of hypoxia on malignant phenotypes (cell proliferation, invasion and anchorage independent growth) in LNCaP and PC-3 prostate cancer cells and 2) assess how over-expression of choline kinase in hypoxic prostate cancer cells affects their malignant phenotypes.

Our results demonstrate that hypoxia affects malignant phenotype of prostate cancer cells depending on their disease progression stage. In terms of regulation of choline phosphorylation, it seems that reduced choline phosphorylation rate in late stage PC-3 cells is indeed a survival response to stressful hypoxic environment. Although, a mechanism to reduce choline phosphorylation exists in the early stage LNCaP cells, they are more tolerant to high choline kinase activity in hypoxic conditions than late stage PC-3 cells.

3. Materials and Methods

3.1. Material

ATCC, Manassas, VA	PC-3 and LNCaP prostate cancer cells RPMI-1640 medium PBS Fetal bovine serum 0.25% Trypsin-EDTA
Eppendorf, Westbury, NY	Centrifuge 5415R
Sigma, St. Louis, MO	Sodium Pentobarbital, Streptomycin, NaOH, SDS, RIPA lysis buffer, protease inhibitor cocktail, DMOG, chloroform, methanol, urea, sulfuric acid, acetonitrile, ammonium acetate, penicillin, scintillation cocktail, glacial acetic acid, HEPES , Triton X-100, EDTA, Bovine Adult Serum, N-tosyl-Lphenylalanine chloromethyl ketone (TPCK), trypsin inhibitor, leupeptin, DTT, PMSF), Tris, HCl, ATP, $MgCl_2$, choline
Waters, Milford, MA	HPLC system
Ruskinn Technologies, Bridgend, UK	Invivo work station
GE Healthcare (Amersham Biosciences), Piscataway, NJ	[^{3}H]choline

3.2. Over-expression of choline kinase

Cells were cultured in RPMI medium supplemented with 10% (v/v) fetal bovine serum (ATCC), 100 units/ml penicillin, and 0.1 mg/ml streptomycin. Cells were grown at 37°C in a humidified incubator with a gas phase of 5% CO_2. The

cells lines were transduced with the retrovirus (pHAGE-CMV-CHKA-ZsGreen-W) or control retrovirus (pHAGE-CMV-MCS-ZsGreen-W) containing medium mixed with 8 µg/ml Polybrene (SIGMA). The retroviruses were created by Dr. Jeng-Shin Lee, Dana-Farber / Harvard Cancer Center.

3.3. Measurement of population doubling time

Cells were trypsinized and suspended in a known volume of medium. The cell suspension was diluted 1000 fold with balanced electrolyte solution. Cells were counted in the diluted suspension using a particle counter. Doubling time was calculated using the formula DT (days) = T x 0.693 / ln (Nf / Ni), where DT is time needed to double a cell population, T is the incubation time in days, Ni is the cell number at the beginning of the incubation time and Nf is the cell number at the end of the incubation time.

3.4. Colony formation assay

Cells (0.5×10^4) were mixed with 1 ml of RPMI 1640 medium containing 0.7% low melting agarose and 10% FBS and then plated on the bottom layer containing RPMI 1640 medium, and 0.8% low melting agarose with 10% FBS in each well of a six-well plate. The top agarose layer was overlaid with 1ml RPMI1640 medium with 10% FBS. The overlay medium was changed every 2 days. After cultured for 21 days in normoxia (21% O_2) or hypoxia (1% O_2), colonies were counted after staining with 0.005% crystal violet.

3.5. Cell invasion assay

Migration/Invasion assay was performed using BioCoat Tumor Invasion Systems (BD Bioscienes) according to manufacturer's protocol. Invasion assay involved BD Falcon HTS FluoroBlok 24-Multiwell Insert System (8 µm) with BD Matrigel Matrix. Migration assay involved uncoated HTS FluoroBlok 24-Multiwell Insert System (8 µm) without BD Matrigel Matrix. PC-3 and LNCaP cells were grown in RPMI 1640 medium supplemented with 10% FBS. Cell suspensions were prepared by trypsinizing the monolayer and resuspending in RPMI 1640 without FBS at 1 x 10^5 cells/ml. The insert plates were prepared by rehydrating the BD Matrigel™ Matrix coating with phosphate buffered saline for two hours at 37°C. The rehydration solution was carefully removed, 0.75 ml RPMI-1640 containing chemoattractant (10% FBS) was added to the plate well, and 0.5 ml of cell suspension (5 x 10^4) was added to each insert well. Uncoated insert plates, included as migration controls, were used without rehydration. This setup was incubated for 48 hours in normoxia (21% O_2) or hypoxia (1% O_2). Following incubation, the medium was removed from upper chamber and entire insert plate was transferred to a second 24-well plate containing 0.5 ml/well of 4 µg/ml Calcein AM (SIGMA) in Hanks buffered saline (SIGMA). The plates were incubated for one hour at 37°C and read in a fluorescence plate reader at excitation wavelength (ex) of 485 nm and emission wavelength (em) of 530 nm without further manipulation. Only labeled cells that pass through the BD Matrigel Matrix layer and the membrane were detected by fluorescence.

3.6. Statistical analysis

Student's t-test was applied for statistical evaluation and a P-value <0.05 was considered significant. Results are presented as means ± standard deviation.

4. Results

4.1 Effect of over-expression of choline kinase on choline uptake

Cells over-expressing choline kinase, PC-3 hChKα$^+$ and LNCaP hChKα$^+$ showed the expected increase in choline uptake as compared to PC-3 and LNCaP cells due to increased trapping of choline as phosphocholine (Figure 26).

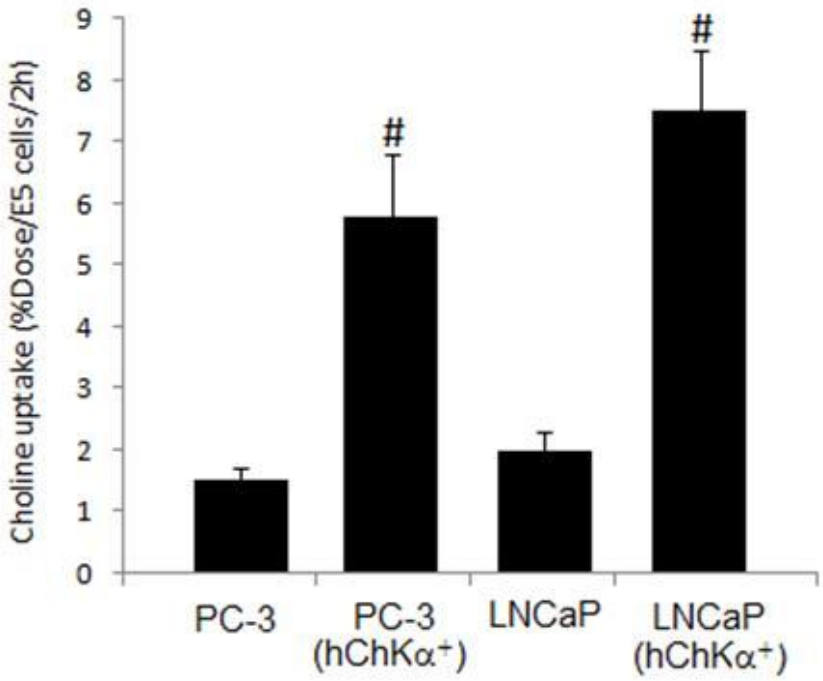

Figure 26. Effect of over-expression of hChKα on choline uptake in prostate cancer cells. # $p < 0.05$ Vs values in control cells not over-expressing hChKα using unpaired t-test.

4.2. Effect of over-expression of choline kinase and hypoxia on population doubling time

Over-expression of choline kinase slightly increased population doubling time of normoxic PC-3 cells but caused a non-significant decrease in population doubling time of normoxic LNCaP cells (Figure 27). Hypoxia caused a decrease in cellular proliferation in all cases except for LNCaP hChKα$^+$ cells. Decrease was more pronounced in PC-3 hChKα$^+$ cells than other cells.

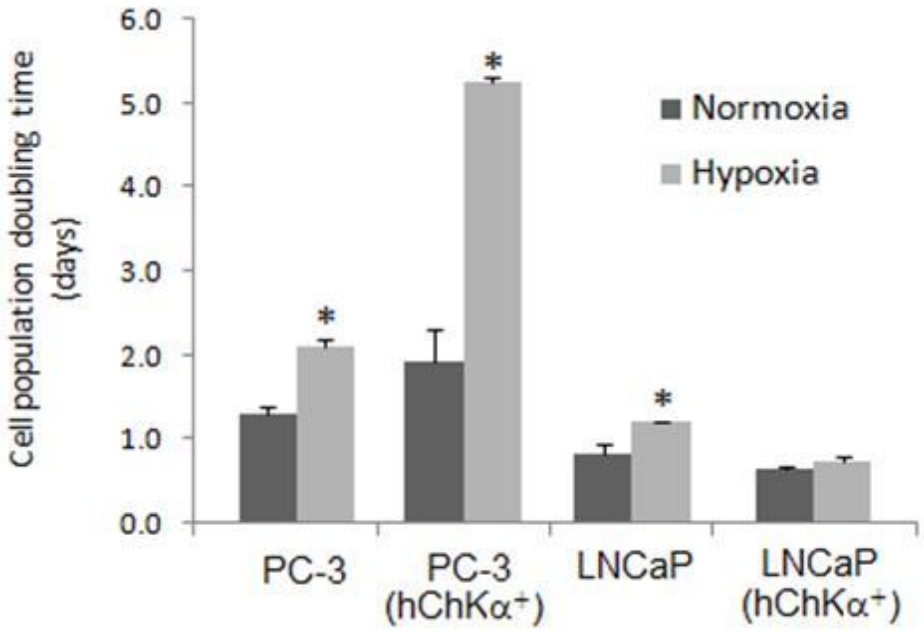

Figure 27. Effect of hypoxia (1% O_2, 24h) and over-expression of hChkα on cell population doubling time of prostate cancer cells. * $p<0.05$ values of hypoxia versus normoxia

4.3. Effect of over-expression of choline kinase on cancer cell morphology

PC-3 cells are strongly adherent cell line that grows as confluent layer of cells with no empty space between the cells whereas LNCaP cells are loosely

adherent cell line growing in clusters with lot of empty space between the clusters. LNCaP cells are more elongated than PC-3 cells. Over-expression of choline kinase had a pronounced effect on cell morphology and growth pattern of prostate cancer cells (Figure 28). Although cell shape and growth pattern of PC-3 hChKα$^+$ cells was not so different from parent PC-3 cells, LNCaP hChKα$^+$ were more like PC-3 cells in shape and growth pattern as compared to parent LNCaP cells. LNCaP hChKα$^+$ were not as elongated as parent LNCaP cells and were more like PC-3 cells. Like PC-3 cells, LNCaP hChKα$^+$ grew as confluent layer of cells as opposed to parent LNCaP cells that grew in clusters.

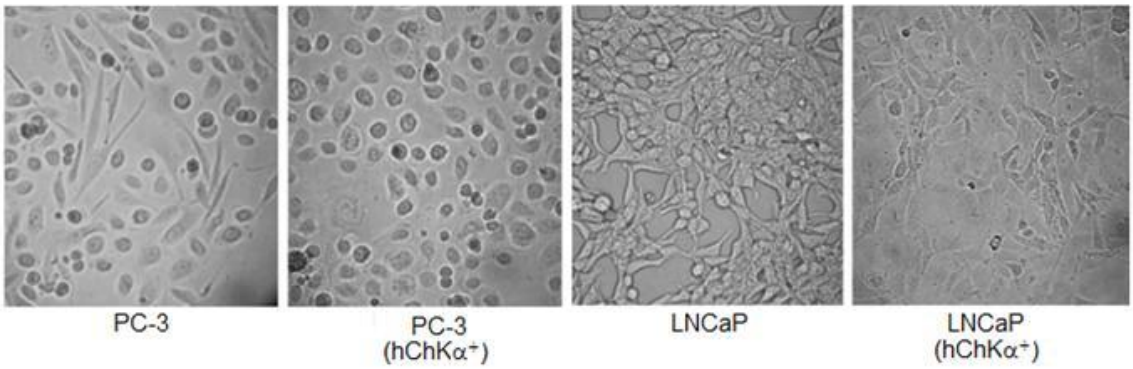

Figure 28. Effect of over-expression of hChKα on cell morphology of prostate cancer cells.

4.4. Effect of over-expression of choline kinase and hypoxia on anchorage independent growth

In this assay, the cells exhibiting anchorage independent growth form colonies in soft agar medium. LNCaP cells have typically a higher proliferation rate than PC-3 cells. This influenced the colony formation assay where LNCaP

was able to form more prominent colonies than PC-3 cells in semi-solid agar medium. Over-expression of choline kinase significantly increased the ability of LNCaP cells to grow in soft agar which was evident from the significant increase of colony forming units of LNCaP hChKα^{+} cells versus parent LNCaP cells (Figure 29). Hypoxia significantly decreased the number and size of colony forming units of LNCaP and LNCaP hChKα^{+} cells (Figure 29).

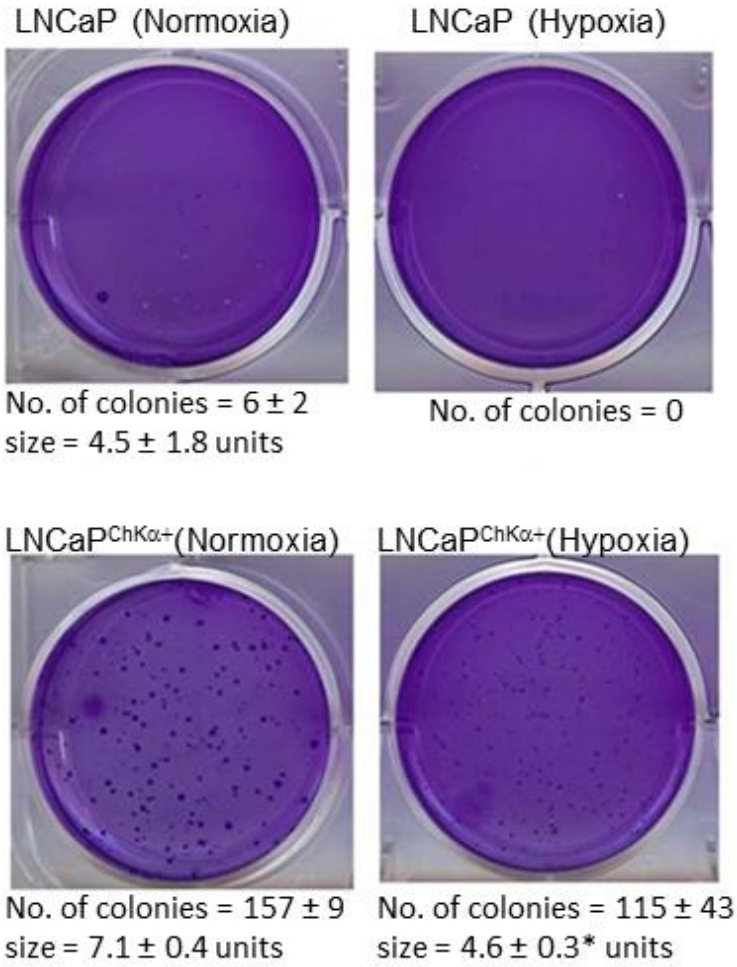

Figure 29. Effect of over-expression of hChKα on anchorage independent growth of LNCaP prostate cancer cells.

4.5. Effect of over-expression of choline kinase and hypoxia on invasion potential of prostate cancer cells

Hypoxia had a positive effect on invasion potential of prostate cancer cells (Figure 30). In the present study, PC-3 cells showed a modest increase in invasion potential in hypoxia (1% O_2) whereas LNCaP cells showed a 9-fold increase in invasion potential in response to hypoxia. In late stage, PC-3 prostate cancer cells, over-expression of choline kinase caused a modest decrease in cell invasion potential in both normoxia and hypoxia. Whereas in early stage, LNCaP prostate cancer cells, over-expression of choline kinase dramatically increased invasion potential. In normoxia, over-expression of choline kinase resulted in transformation of LNCaP from a non-invasive cell line to a moderately invasive cell line. (Figure 30) The 25-fold increase in invasion was more than the one caused due to hypoxia. In PC-3 hChKα$^+$ and LNCaP hChKα$^+$ cells, hypoxia did not significantly increase the invasion potential, although an increasing trend was observed.

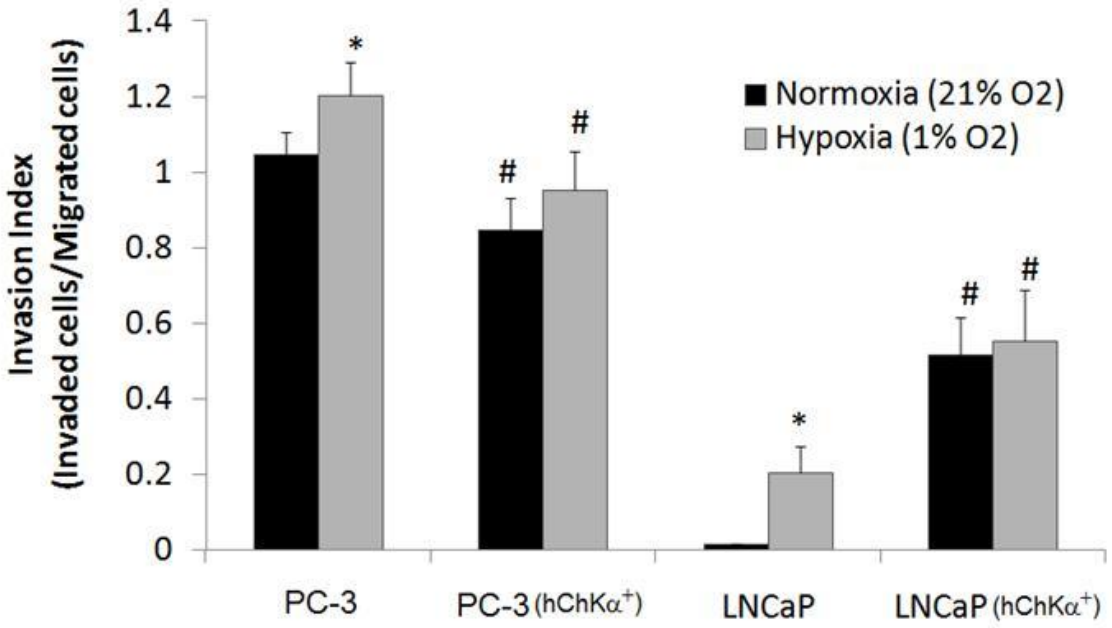

Figure 30. Effect of hypoxia and over-expression of hChKα on invasion potential of PC-3 and LNCaP prostate cancer cells. *$p<0.05$ values for hypoxia Vs normoxia and # $p<0.05$ values for PC-3 (hChKα$^+$) and LNCaP(hChKα$^+$) Vs PC-3 and LNCaP.

4.6. Effect of over-expression of choline kinase and hypoxia on expression of pro-invasion factor, urokinase plasminogen activator (uPa)

The expression pattern of uPA correlated with the invasion pattern of prostate cancer cells in response to over-expression of choline kinase and hypoxia (Figure 31). Upon hypoxic exposure there was significant increase in uPA expression in LNCaP but no significant difference was observed between normoxic and hypoxic PC-3 cells (data not shown). In LNCaP cells, over-expression of choline kinase increased uPA expression in normoxia and this increased uPA expression was also maintained in hypoxia.

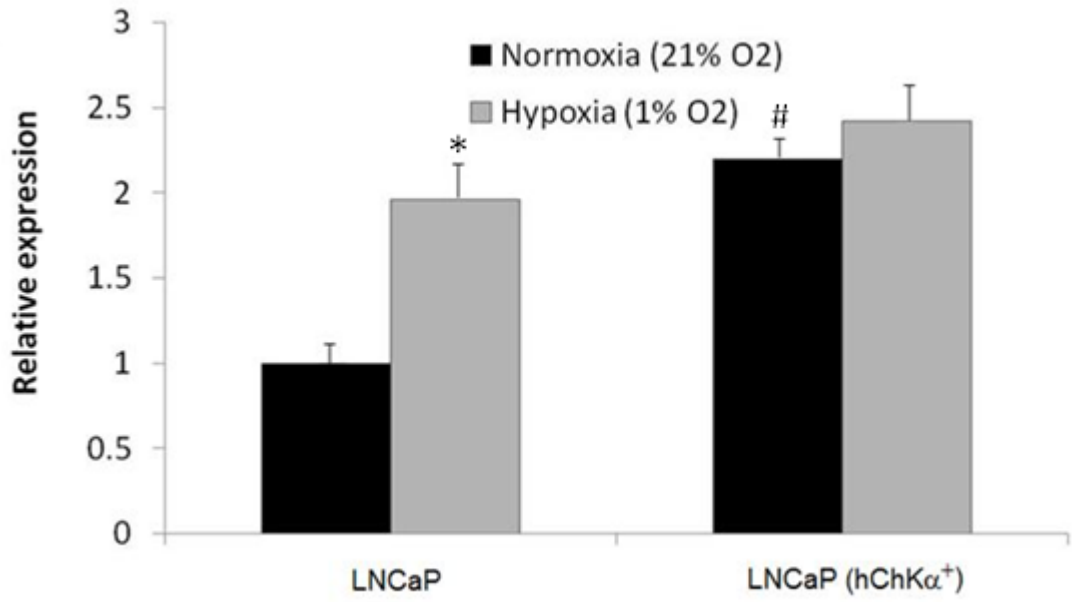

Figure 31. Effect of hypoxia and over-expression of hChKα on expression of promigratory factor, uPA in LNCaP prostate cancer cells. * $p < 0.05$ Vs values in normoxia using unpaired t-test. Relative expression represents expression normalized to expression in normoxic LNCaP cells.

5. Discussion

Decreased choline phosphorylation and down-regulation of choline kinase in hypoxic cancer cells is well reported but its survival advantage in terms of its effect on malignant phenotypes of hypoxic cancer cells is at present not known. In our study we addressed this issue by generating stable prostate cancer cell lines of LNCaP and PC-3 cells that over-express choline kinase independent of normoxic and hypoxic conditions. This allowed us to examine the relationship of malignant phenotypes to choline kinase expression and hypoxia in the two prostate cancer cell lines.

The original hypothesis of this study was that over-expression of choline kinase will have a positive effect on proliferation rate of cancer cells. This was

based on the fact that over-expression of choline kinase is often associated with malignancy and high proliferation. Recently, correlation studies have shown that hypoxia and increased choline kinase activity exist together in tumors (Glunde et al, 2008). It was proposed that together they should be promoting malignancy. However the data obtained in the present study showed that response to over-expression of choline kinase and hypoxia depends on the disease stage of cancer. Over-expression of choline kinase was not favored by late stage representing PC-3 prostate cancer cells as it caused a decrease in cellular proliferation which was more significant in hypoxia. On the other hand, LNCaP cells that represent early stage prostate cancer responded favorably to increased choline kinase activity as seen from increases in cellular proliferation. Over-expression of choline kinase also enhanced anchorage independent growth of LNCaP cells, whereas hypoxia significantly decreased the size of the colonies probably due to decrease in proliferation rate. In late stage PC-3 cells, hypoxia together with increased choline kinase activity profoundly decreased cellular proliferation.

Hypoxia and choline kinase not only modulate proliferation rate of cancer cells but also influence their invasion potential. Hypoxia had a positive effect on invasion potential of PC-3 and LNCaP prostate cancer cells consistent with earlier reports that showed increased invasion upon hypoxic exposure in breast cancer cell lines, MDA-MB-231 and MDA-MB-435 (Graham et al., 1999) and colon cancer cell line, HCT116 (Krishnamachary et al., 2003). In the present study, PC-3 prostate cancer cell line showed a modest increase in invasion

potential in hypoxia (1% O_2) whereas LNCaP prostate cancer cells showed a more pronounced response to hypoxia. LNCaP cells were non-invasive in normoxic condition but hypoxia caused LNCaP to attain invasive characteristic. In this regard, our results contradict an earlier study where hypoxia decreased cell invasion of PC-3 cells in as low as 12h of exposure (Ackerstaff et al., 2007). The reason for this disagreement is not clear but there were methodological differences in performance of the invasion assay. In general, cell invasion assays employ two chambers separated by a reconstituted basement membrane (matrigel). There are two essential requirements for this assay, 1) directed cell movement from upper chamber to lower chamber through the matrigel and 2) degradation of matrigel barrier by invading cells. Ours and other studies (Graham et al., 1999; Krishnamachary et al., 2003) that showed a positive effect of hypoxia on cell invasion followed the widely used serum gradient directed cell movement in the invasion assay. In this methodology, the upper chamber contains cancer cells in serum free medium and lower chamber contains medium with 10% serum. The serum in the lower chamber acts as chemoattractant promoting directed movement of cells from upper chamber to lower chamber. This methodology closely mimics the *in vivo* conditions where chemo-attractant based gradients between primary tumors, circulating blood and metastatic sites are important factors that contribute to cellular invasion (Moore et al., 2001). The contradicting report employed a perfusion based cell invasion system in which cell movement was directed not by a serum gradient but by the flow of perfused medium which was from the upperchamber to the lower

chamber (Ackerstaff et al., 2007). Serum is an important factor in invasion assays. This is evident from studies with choriocarcinoma HTR-8/SVneo cells performed in the absence of serum showed a negative effect of hypoxia on invasion potential of these cells (Kilburn et al., 2000) but in a different study, the invasion potential of HTR-8/SVneo cells was significantly increased by hypoxia in the presence of a serum gradient (Graham et al., 1998). Similar differences in invasion response to hypoxia due to serum gradient were reported in the breast cancer cell line MDA-MB-231 (Munoz-Najar et al., 2006). Finally, another methodological difference in the contradicting report is that their calculated invasion potential (invasion index) reflected both cell migration and matrigel physical degradation caused by invading cells. This differed from the invasion index that I measured which reflected only cell invasion.

Promigratory factor, uPA is a serine protease that converts plasminogen into plasmin, a broadly acting protease that degrades several extracellular matrix proteins. Consistent with its role in cancer progression, multiple groups have shown that high levels of uPA in primary breast cancers are independently associated with metastasis (Foekens et al., 1992). uPA level indicates invasion potential of prostate cancer cell line evident from high uPA levels in highly invasive, PC-3 cells and absence of uPA in non-invasive LNCaP cells (Pentyala et al., 1998). In the case of PC-3 prostate cancer cells, PC-3 transfected with a mutant inactive form of uPA, displayed reduced metastatic ability when inoculated into nude mice, suggesting involvement of uPA in cell invasiveness (Crowley et al., 1993). In present study, the expression pattern of uPA correlated

with the invasion pattern seen in hypoxic prostate cancer cells. Hypoxia and over-expression of choline kinase caused significant increase in uPA expression in LNCaP but no significant difference was observed in PC-3 cells. These observations suggest that hypoxia and choline kinase affects these two prostate cancer cell lines in different ways in terms of modulating cell uPA expression. It is possible that the highly invasive PC-3 cells have little room for further increase in invasion potential while the relatively non-invasive LNCaP cells have more potential of being modulated. Cells that are noninvasive can be become invasive with changes in microenvironment. Our present work provides first evidence that hypoxia and ChKα expression could be affecting malignant phenotypes of prostate cancer cells depending on their stage in cancer disease progression.

CONCLUSIONS

Present work clarifies the status of choline metabolism and regulation of choline kinase expression in hypoxic cancer cells. In addition it presents preliminary results showing that inhibition of choline kinase in hypoxic cancer cells might have a survival advantage depending on disease stage of cancer. In the cancer cells that were studied, 9L glioma cells, PC-3 and LNCaP prostate cancer cells, it was observed that hypoxia universally inhibits choline uptake /phosphorylation in all cancer cells independent of their origin. Inhibition of choline phosphorylation was strong in some cells (PC-3) and modest in others (9L glioma and LNCaP). Response in cultured cancer cells were further confirmed when inhibition of choline phosphorylation was also seen in hypoxic 9L tumor animal model. Decreased choline phosphorylation resulted in transient uptake of choline radiotracers in cultured cancer cells and 9L tumors suggesting potential problem in using choline as a biomarker for cancers in hypoxic microenvironment.

To investigate the mechanism behind decrease in choline phosphorylation, steady state levels of choline metabolites were measured and choline kinase catalyzed choline phosphorylation step was found to be rate-limiting in PC-3 cells. This suggested that modulation in choline kinase levels can alter choline metabolism in hypoxic cancer cells. Expression and activity assays for choline kinase revealed that choline kinase expression is down-regulated in hypoxia.

This regulation involved transcriptional level mediation by HIF1 at the conserved HRE7 site in choline kinase promoter.

The mechanism behind this HIF-1 mediated response and reason for inhibition of choline kinase in hypoxic cells is not known but preliminary experiments suggest that this inhibition might have a survival advantage to cancer cells depending on their stage in cancer disease progression. Over-expression of choline kinase in hypoxic PC-3 cells was not well tolerated in our study as it resulted in significant reduction in invasion potential and slower population doubling rate. Further study showed that in contrast to highly invasive PC-3, in non-invasive LNCaP cells, over-expression of choline kinase was tolerated in hypoxia. Over-expression of choline kinase significantly increased invasion potential of LNCaP cells with no significant difference in population doubling time. These results suggests that tumor microenvironment are important for progression of early-stage, androgen-dependent LNCaP prostate cancer cells but confer little survival advantage in undifferentiated, androgen-independent PC-3 prostate cancer cells.

REFERENCES

Ackerstaff, E., D. Artemov, et al. (2007). Hypoxia and the presence of human vascular endothelial cells affect prostate cancer cell invasion and metabolism. Neoplasia 9(12): 1138-1151.

Ackerstaff, E., K. Glunde, et al. (2003). Choline phospholipid metabolism: a target in cancer cells? J Cell Biochem 90(3): 525-533.

Anastasiadis, A. G., B. C. Stisser, et al. (2002). Tumor hypoxia and the progression of prostate cancer. Curr Urol Rep 3(3): 222-228.

Aoyama, C., H. Liao, et al. (2004). Structure and function of choline kinase isoforms in mammalian cells. Prog Lipid Res 43(3): 266-281.

Aoyama, C., K. Nakashima, et al. (1998). Complementary DNA sequence for a 42 kDa rat kidney choline/ethanolamine kinase. Biochim Biophys Acta 1390(1): 1-7.

Aoyama, C., A. Ohtani, et al. (2002). Expression and characterization of the active molecular forms of choline/ethanolamine kinase-alpha and -beta in mouse tissues, including carbon tetrachloride-induced liver. Biochem J 363(Pt 3): 777-784.

Bouwman, P. and S. Philipsen (2002). Regulation of the activity of Sp1-related transcription factors. Mol Cell Endocrinol 195(1-2): 27-38.

Burckhardt, G. and N. A. Wolff (2000). Structure of renal organic anion and cation transporters. Am J Physiol Renal Physiol 278(6): F853-866.

Caro, J. (2001). Hypoxia regulation of gene transcription. High Alt Med Biol 2(2): 145-154.

Chen, C., N. Pore, et al. (2001). Regulation of glut1 mRNA by hypoxia-inducible factor-1. Interaction between H-ras and hypoxia. J Biol Chem 276(12): 9519-9525.

Choi, M. G., V. Kurnov, et al. (2005). Phosphorylation of the yeast choline kinase by protein kinase C. Identification of Ser25 and Ser30 as major sites of phosphorylation. J Biol Chem 280(28): 26105-26112.

Chua, B. T., D. Gallego-Ortega, et al. (2009). Regulation of Akt(ser473) phosphorylation by choline kinase in breast carcinoma cells. Mol Cancer 8: 131.

Cimitan, M., R. Bortolus, et al. (2006). [(18)F]fluorocholine PET/CT imaging for the detection of recurrent prostate cancer at PSA relapse: experience in 100 consecutive patients. Eur J Nucl Med Mol Imaging.

Coleman, R., T. DeGrado, et al. (2000). 9:30-9:45. Preliminary Evaluation of F-18 Fluorocholine (FCH) as a PET Tumor Imaging Agent. Clin Positron Imaging 3(4): 147.

Crowley, C. W., R. L. Cohen, et al. (1993). Prevention of metastasis by inhibition of the urokinase receptor. Proc Natl Acad Sci U S A 90(11): 5021-5025.

Cuadrado, A., A. Carnero, et al. (1993). Phosphorylcholine: a novel second messenger essential for mitogenic activity of growth factors. Oncogene 8(11): 2959-2968.

DeGrado, T. R., S. W. Baldwin, et al. (2001). Synthesis and evaluation of (18)F-labeled choline analogs as oncologic PET tracers. J Nucl Med 42(12): 1805-1814.

DeGrado, T. R., R. E. Coleman, et al. (2001). Synthesis and evaluation of 18F-labeled choline as an oncologic tracer for positron emission tomography: initial findings in prostate cancer. Cancer Res 61(1): 110-117.

Eltzschig, H. K., P. Abdulla, et al. (2005). HIF-1-dependent repression of equilibrative nucleoside transporter (ENT) in hypoxia. J Exp Med 202(11): 1493-1505.

Elvidge, G. P., L. Glenny, et al. (2006). Concordant regulation of gene expression by hypoxia and 2-oxoglutarate-dependent dioxygenase inhibition: the role of HIF-1alpha, HIF-2alpha, and other pathways. J Biol Chem 281(22): 15215-15226.

Finkelstein, J. D., J. J. Martin, et al. (1982). Regulation of the betaine content of rat liver. Arch Biochem Biophys 218(1): 169-173.

Firth, J. D., B. L. Ebert, et al. (1995). Hypoxic regulation of lactate dehydrogenase A. Interaction between hypoxia-inducible factor 1 and cAMP response elements. J Biol Chem 270(36): 21021-21027.

Fiscus, W. G. and W. C. Schneider (1966). The role of phospholipids in stimulating phosphorylcholine cytidyltransferase activity. J Biol Chem 241(14): 3324-3330.

Florin, L., L. Hummerich, et al. (2004). Identification of novel AP-1 target genes in fibroblasts regulated during cutaneous wound healing. Oncogene 23(42): 7005-7017.

Foekens, J. A., M. Schmitt, et al. (1992). Prognostic value of urokinase-type plasminogen activator in 671 primary breast cancer patients. Cancer Res 52(21): 6101-6105.

Gallego-Ortega, D., A. Ramirez de Molina, et al. (2009). Differential role of human choline kinase alpha and beta enzymes in lipid metabolism: implications in cancer onset and treatment. PLoS One 4(11): e7819.

Garcia-Perez, A. and M. B. Burg (1991). Role of organic osmolytes in adaptation of renal cells to high osmolality. J Membr Biol 119(1): 1-13.

Glunde, K., T. Shah, et al. (2008). Hypoxia regulates choline kinase expression through hypoxia-inducible factor-1 alpha signaling in a human prostate cancer model. Cancer Res 68(1): 172-180.

Graham, C. H., T. E. Fitzpatrick, et al. (1998). Hypoxia stimulates urokinase receptor expression through a heme protein-dependent pathway. Blood 91(9): 3300-3307.

Graham, C. H., J. Forsdike, et al. (1999). Hypoxia-mediated stimulation of carcinoma cell invasiveness via upregulation of urokinase receptor expression. Int J Cancer 80(4): 617-623.

Groenman, F. A., M. Rutter, et al. (2007). Effect of chemical stabilizers of hypoxia-inducible factors on early lung development. Am J Physiol Lung Cell Mol Physiol 293(3): L557-567.

Hara, M. (1987). [Clinical studies on cefoperazone and polymyxin B for the treatment of infections in patients with hematological malignancies]. Jpn J Antibiot 40(9): 1639-1643.

Hara, T. (2001). 18F-fluorocholine: a new oncologic PET tracer. J Nucl Med 42(12): 1815-1817.

Hara, T., A. Bansal, et al. (2006). Effect of hypoxia on the uptake of [methyl-3H]choline, [1-14C] acetate and [18F]FDG in cultured prostate cancer cells. Nucl Med Biol 33(8): 977-984.

Hara, T., N. Kosaka, et al. (1998). PET imaging of prostate cancer using carbon-11-choline. J Nucl Med 39(6): 990-995.

Hara, T., N. Kosaka, et al. (2002). Development of (18)F-fluoroethylcholine for cancer imaging with PET: synthesis, biochemistry, and prostate cancer imaging. J Nucl Med 43(2): 187-199.

Hara, T., N. Kosaka, et al. (1997). PET imaging of brain tumor with [methyl-11C]choline. J Nucl Med 38(6): 842-847.

Heinisch, M., A. Dirisamer, et al. (2006). Positron emission tomography/computed tomography with F-18-fluorocholine for restaging of prostate cancer patients: meaningful at PSA < 5 ng/ml? Mol Imaging Biol 8(1): 43-48.

Henriksen, G., M. Herz, et al. (2004). Synthesis and preclinical evaluation of the choline transport tracer deshydroxy-[18F]fluorocholine ([18F]dOC). Nucl Med Biol 31(7): 851-858.

Hess, J., P. Angel, et al. (2004). AP-1 subunits: quarrel and harmony among siblings. J Cell Sci 117(Pt 25): 5965-5973.

Infante, J. P. (1977). Rate-limiting steps in the cytidine pathway for the synthesis of phosphatidylcholine and phosphatidylethanolamine. Biochem J 167(3): 847-849.

Infante, J. P. and J. E. Kinsella (1978). A novel method for determining equilibrium constants. CTP:phosphorylcholine cytidyltransferase. Biochim Biophys Acta 526(2): 440-449.

Ishidate, K. (1997). Choline/ethanolamine kinase from mammalian tissues. Biochim Biophys Acta 1348(1-2): 70-78.

Ishidate, K., K. Furusawa, et al. (1985). Complete co-purification of choline kinase and ethanolamine kinase from rat kidney and immunological evidence for both kinase activities residing on the same enzyme protein(s) in rat tissues. Biochim Biophys Acta 836(1): 119-124.

Ishidate, K., K. Iida, et al. (1985). Evidence for the existence of multiple forms of choline (ethanolamine) kinase in rat tissues. Biochim Biophys Acta 833(1): 1-8.

Ishidate, K. and Y. Nakazawa (1992). Choline/ethanolamine kinase from rat kidney. Methods Enzymol 209: 121-134.

Jacobs, R. L., S. Lingrell, et al. (2007). Inhibition of hepatic phosphatidylcholine synthesis by 5-aminoimidazole-4-carboxamide-1-beta-4-ribofuranoside is independent of AMP-activated protein kinase activation. J Biol Chem 282(7): 4516-4523.

Jenkins, W. T., S. M. Evans, et al. (2000). Hypoxia and necrosis in rat 9L glioma and Morris 7777 hepatoma tumors: comparative measurements using EF5 binding and the Eppendorf needle electrode. Int J Radiat Oncol Biol Phys 46(4): 1005-1017.

Jimenez, B., L. del Peso, et al. (1995). Generation of phosphorylcholine as an essential event in the activation of Raf-1 and MAP-kinases in growth factors-induced mitogenic stimulation. J Cell Biochem 57(1): 141-149.

Kaighn, M. E., K. S. Narayan, et al. (1979). Establishment and characterization of a human prostatic carcinoma cell line (PC-3). Invest Urol 17(1): 16-23.

Kallinowski, F., K. H. Schlenger, et al. (1989). Blood flow, metabolism, cellular microenvironment, and growth rate of human tumor xenografts. Cancer Res 49(14): 3759-3764.

Katz-Brull, R. and H. Degani (1996). Kinetics of choline transport and phosphorylation in human breast cancer cells; NMR application of the zero trans method. Anticancer Res 16(3B): 1375-1380.

Katz-Brull, R., D. Seger, et al. (2002). Metabolic markers of breast cancer: enhanced choline metabolism and reduced choline-ether-phospholipid synthesis. Cancer Res 62(7): 1966-1970.

Kent, C. (2005). Regulatory enzymes of phosphatidylcholine biosynthesis: a personal perspective. Biochim Biophys Acta 1733(1): 53-66.

Kilburn, B. A., J. Wang, et al. (2000). Extracellular matrix composition and hypoxia regulate the expression of HLA-G and integrins in a human trophoblast cell line. Biol Reprod 62(3): 739-747.

Kim, K. H., D. R. Voelker, et al. (1998). Expression, purification, and characterization of choline kinase, product of the CKI gene from Saccharomyces cerevisiae. J Biol Chem 273(12): 6844-6852.

Krishnamachary, B., S. Berg-Dixon, et al. (2003). Regulation of colon carcinoma cell invasion by hypoxia-inducible factor 1. Cancer Res 63(5): 1138-1143.

Kwee, S. A., M. N. Coel, et al. (2004). Combined use of F-18 fluorocholine positron emission tomography and magnetic resonance spectroscopy for brain tumor evaluation. J Neuroimaging 14(3): 285-289.

Kwee, S. A., M. N. Coel, et al. (2005). Prostate cancer localization with 18fluorine fluorocholine positron emission tomography. J Urol 173(1): 252-255.

Kwee, S. A., H. Wei, et al. (2006). Localization of Primary Prostate Cancer with Dual-Phase 18F-Fluorocholine PET. J Nucl Med 47(2): 262-269.

Langeler, E. G., C. J. van Uffelen, et al. (1993). Effect of culture conditions on androgen sensitivity of the human prostatic cancer cell line LNCaP. Prostate 23(3): 213-223.

Liu, L., T. P. Cash, et al. (2006). Hypoxia-induced energy stress regulates mRNA translation and cell growth. Mol Cell 21(4): 521-531.

Lockman, P. R. and D. D. Allen (2002). The transport of choline. Drug Dev Ind Pharm 28(7): 749-771.

Lusska, A., E. Shen, et al. (1993). Protein-DNA interactions at a dioxin-responsive enhancer. Analysis of six bona fide DNA-binding sites for the liganded Ah receptor. J Biol Chem 268(9): 6575-6580.

Malito, E., N. Sekulic, et al. (2006). Elucidation of human choline kinase crystal structures in complex with the products ADP or phosphocholine. J Mol Biol 364(2): 136-151.

Martel, F., D. Grundemann, et al. (2001). Apical uptake of organic cations by human intestinal Caco-2 cells: putative involvement of ASF transporters. Naunyn Schmiedebergs Arch Pharmacol 363(1): 40-49.

Moore, M. A. (2001). The role of chemoattraction in cancer metastases. Bioessays 23(8): 674-676.

Movsas, B., J. D. Chapman, et al. (2000). Increasing levels of hypoxia in prostate carcinoma correlate significantly with increasing clinical stage and patient age: an Eppendorf pO(2) study. Cancer 89(9): 2018-2024.

Movsas, B., J. D. Chapman, et al. (1999). Hypoxic regions exist in human prostate carcinoma. Urology 53(1): 11-18.

Munoz-Najar, U. M., K. M. Neurath, et al. (2006). Hypoxia stimulates breast carcinoma cell invasion through MT1-MMP and MMP-2 activation. Oncogene 25(16): 2379-2392.

Newsholme, E. A. and B. Crabtree (1973). Metabolic aspects of enzyme activity regulation. Symp Soc Exp Biol 27: 429-460.

Nguyen, S. V. and W. C. Claycomb (1999). Hypoxia regulates the expression of the adrenomedullin and HIF-1 genes in cultured HL-1 cardiomyocytes. Biochem Biophys Res Commun 265(2): 382-386.

Okino, S. T., C. H. Chichester, et al. (1998). Hypoxia-inducible mammalian gene expression analyzed in vivo at a TATA-driven promoter and at an initiator-driven promoter. J Biol Chem 273(37): 23837-23843.

Peisach, D., P. Gee, et al. (2003). The crystal structure of choline kinase reveals a eukaryotic protein kinase fold. Structure 11(6): 703-713.

Pelech, S. L. and D. E. Vance (1984). Regulation of phosphatidylcholine biosynthesis. Biochim Biophys Acta 779(2): 217-251.

Pentyala, S. N., T. C. Whyard, et al. (1998). Androgen induction of urokinase gene expression in LNCaP cells is dependent on their interaction with the extracellular matrix. Cancer Lett 130(1-2): 121-126.

Philipsen, S. and G. Suske (1999). A tale of three fingers: the family of mammalian Sp/XKLF transcription factors. Nucleic Acids Res 27(15): 2991-3000.

Price, D. T., R. E. Coleman, et al. (2002). Comparison of [18 F]fluorocholine and [18 F]fluorodeoxyglucose for positron emission tomography of androgen dependent and androgen independent prostate cancer. J Urol 168(1): 273-280.

Ramirez de Molina, A., D. Gallego-Ortega, et al. (2008). Choline kinase as a link connecting phospholipid metabolism and cell cycle regulation: implications in cancer therapy. Int J Biochem Cell Biol 40(9): 1753-1763.

Ramirez de Molina, A., D. Gallego-Ortega, et al. (2005). Choline kinase is a novel oncogene that potentiates RhoA-induced carcinogenesis. Cancer Res 65(13): 5647-5653.

Ramirez de Molina, A., R. Gutierrez, et al. (2002). Increased choline kinase activity in human breast carcinomas: clinical evidence for a potential novel antitumor strategy. Oncogene 21(27): 4317-4322.

Ramirez de Molina, A., A. Rodriguez-Gonzalez, et al. (2002). Overexpression of choline kinase is a frequent feature in human tumor-derived cell lines and in lung, prostate, and colorectal human cancers. Biochem Biophys Res Commun 296(3): 580-583.

Ratnam, S. and C. Kent (1995). Early increase in choline kinase activity upon induction of the H-ras oncogene in mouse fibroblast cell lines. Arch Biochem Biophys 323(2): 313-322.

Reinhardt, R. R., L. Wecker, et al. (1984). Kinetic mechanism of choline kinase from rat striata. J Biol Chem 259(12): 7446-7452.

Riddle, S. R., A. Ahmad, et al. (2000). Hypoxia induces hexokinase II gene expression in human lung cell line A549. Am J Physiol Lung Cell Mol Physiol 278(2): L407-416.

Rodriguez-Gonzalez, A., A. Ramirez de Molina, et al. (2004). Choline kinase inhibition induces the increase in ceramides resulting in a highly specific and selective cytotoxic antitumoral strategy as a potential mechanism of action. Oncogene 23(50): 8247-8259.

Rosenberger, P., J. Khoury, et al. (2007). Identification of vasodilator-stimulated phosphoprotein (VASP) as an HIF-regulated tissue permeability factor during hypoxia. FASEB J 21(10): 2613-2621.

Sarri, E., D. Garcia-Dorado, et al. (2006). Effects of hypoxia, glucose deprivation and acidosis on phosphatidylcholine synthesis in HL-1 cardiomyocytes. CTP:phosphocholine cytidylyltransferase activity correlates with sarcolemmal disruption. Biochem J 394(Pt 1): 325-334.

Schmid, D. T., H. John, et al. (2005). Fluorocholine PET/CT in patients with prostate cancer: initial experience. Radiology 235(2): 623-628.

Semenza, G. L. (1998). Hypoxia-inducible factor 1: master regulator of O2 homeostasis. Curr Opin Genet Dev 8(5): 588-594.

Semenza, G. L. (2000). Expression of hypoxia-inducible factor 1: mechanisms and consequences. Biochem Pharmacol 59(1): 47-53.

Semenza, G. L., B. H. Jiang, et al. (1996). Hypoxia response elements in the aldolase A, enolase 1, and lactate dehydrogenase A gene promoters contain essential binding sites for hypoxia-inducible factor 1. J Biol Chem 271(51): 32529-32537.

Semenza, G. L., P. H. Roth, et al. (1994). Transcriptional regulation of genes encoding glycolytic enzymes by hypoxia-inducible factor 1. J Biol Chem 269(38): 23757-23763.

Shaywitz, A. J. and M. E. Greenberg (1999). CREB: a stimulus-induced transcription factor activated by a diverse array of extracellular signals. Annu Rev Biochem 68: 821-861.

Shinoura, N., M. Nishijima, et al. (1997). Brain tumors: detection with C-11 choline PET. Radiology 202(2): 497-503.

Tadokoro, K., K. Ishidate, et al. (1985). Evidence for the existence of isozymes of choline kinase and their selective induction in 3-methylcholanthrene- or carbon tetrachloride-treated rat liver. Biochim Biophys Acta 835(3): 501-513.

Talbot, J. N., F. Gutman, et al. (2006). PET/CT in patients with hepatocellular carcinoma using [(18)F]fluorocholine: preliminary comparison with [(18)F]FDG PET/CT. Eur J Nucl Med Mol Imaging.

Traut, T. W. (1994). Dissociation of enzyme oligomers: a mechanism for allosteric regulation. Crit Rev Biochem Mol Biol 29(2): 125-163.

Uchida, T. (1994). Regulation of choline kinase R: analyses of alternatively spliced choline kinases and the promoter region. J Biochem 116(3): 508-518.

Vaupel, P., F. Kallinowski, et al. (1989). Blood flow, oxygen and nutrient supply, and metabolic microenvironment of human tumors: a review. Cancer Res 49(23): 6449-6465.

Warden, C. H. and M. Friedkin (1985). Regulation of choline kinase activity and phosphatidylcholine biosynthesis by mitogenic growth factors in 3T3 fibroblasts. J Biol Chem 260(10): 6006-6011.

Wilgram, G. F. and E. P. Kennedy (1963). Intracellular Distribution of Some Enzymes Catalyzing Reactions in the Biosynthesis of Complex Lipids. J Biol Chem 238: 2615-2619.

Wittenberg, J. and A. Kornberg (1953). Choline phosphokinase. J Biol Chem 202(1): 431-444.

Xia, X. and A. L. Kung (2009). Preferential binding of HIF-1 to transcriptionally active loci determines cell-type specific response to hypoxia. Genome Biol 10(10): R113.

Xia, X., M. E. Lemieux, et al. (2009). Integrative analysis of HIF binding and transactivation reveals its role in maintaining histone methylation homeostasis. Proc Natl Acad Sci U S A 106(11): 4260-4265.

Yeo, E. J., Y. S. Chun, et al. (2004). New anticancer strategies targeting HIF-1. Biochem Pharmacol 68(6): 1061-1069.

Yao, E. F. and M. S. Denison (1992). DNA sequence determinants for binding of transformed Ah receptor to a dioxin-responsive enhancer. Biochemistry 31(21): 5060-5067.

Zheng, W., J. Kuhlicke, et al. (2009). Hypoxia inducible factor-1 (HIF-1)-mediated repression of cystic fibrosis transmembrane conductance regulator (CFTR) in the intestinal epithelium. FASEB J 23(1): 204-213.

CURRICULUM VITAE

Aditya Bansal

Education:

Doctor of Philosophy, 10/2010
Indiana University, Indianapolis, Indiana
Major: Biochemistry and Molecular Biology
Minor: Cancer Biology

Master of Science, 12/2005
Indiana University, Indianapolis, Indiana
Major: Biochemistry and Molecular Biology

Master of Science, 7/2001
University of Delhi, Delhi, India
Major: Botany

Bachelor of Science, 7/1999
University of Delhi, Delhi, India
Major: Botany

Professional Background:

Research Assistant, 2001-2003
Department of Biotechnology, GGSIPU, India
(Supervised by: Dr. Ashwani Pareek, Ph.D.)

Research Assistant, 2003-2010
Department of Radiology, Indiana University School of Medicine
(Supervised by: Dr. Timothy R. DeG-rado, Ph.D.)

Awards:

Junior Research Fellowship by Council for Scientific and Industrial Research, New Delhi, India (2001-2002)

Publications:

Bansal A, Wang S, Hara T, Harris RA, DeGrado TR. (2008) Biodisposition and metabolism of [^{18}F]fluorocholine (FCH) in 9L glioma cells and 9L glioma-bearing Fisher rats. European Journal of Nuclear Medicine and Molecular Imaging. 35(6): 1192–1203.

Hara T, **Bansal A**, DeGrado TR. (2006) Effect of hypoxia on the uptake of [methyl-^{3}H]choline, [1-^{14}C] acetate and [^{18}F]FDG in cultured prostate cancer cells. Nuclear Medicine and Biology 33(8):977-84.

Hara T, **Bansal A**, DeGrado TR. (2006) Choline transporter as a novel target for molecular imaging of cancer. Molecular Imaging 5(4):498-509.

Conference Attended:

Bansal A, Wang S, Nazih R, Harris RA, DeGrado TR (2009) Comparison of [^{18}F]Fluorocholine (FCH) Uptake and Perfusion in hypoxic 9L Glioma Tumor Model. J Nucl Med. 50 (Supplement 2):1600

Bansal A, Nazih R, Wang S, Harris RA, DeGrado TR. (2007) Evaluation of [^{18}F]fluoroethylcholine (FECH) in fisher rats bearing hypoxic subcutaneous 9L tumor. Molecular Imaging and Biology

Bansal A, Wang S, Harris RA, Hara T, DeGrado TR. (2006) Biodisposition and metabolism of [^{18}F]fluorocholine (FCH) in cultured 9L glioma cells and subcutaneous 9L tumor model. Molecular Imaging and Biology

Bansal A, Wang S, Sanghani PS, DeGrado TR. (2005) Characterization of human choline kinase as target for PET imaging using positron-labeled choline analogs. Molecular Imaging and Biology

Bansal A, Nazih R, Wang S, Harris RA, DeGrado TR. (2007) Phosphorylation of fluorinated choline analogs (FCAs) by human choline kinase. J Nucl Med. 48 (Supplement 2):19P

Bansal A, Nazih R, Wang S, Harris RA, DeGrado TR. (2007) [^{18}F]Fluoromethylallylcholine (FMAC): Evaluation of a new PET tracer for cancer imaging. J Nucl Med. 48 (Supplement 2):32P

NCBI Submissions:

Kumar M, **Bansal A**, Singla-Pareek SL, Sopory SK and Pareek A (2006) Oryza sativa (indica cultivar-group) hybrid type histidine kinase mRNA, complete cds. NCBI Accession # DQ248962

Bansal A, Singla-Pareek SL, Reddy MK, Sopory SK and Pareek A (2003) Oryza sativa (indica cultivar-group) histidine kinase (HK1) mRNA, partial cds. NCBI Accession # AY211488

Bansal A, Singla-Pareek S.L., Reddy M.K., Sopory S.K. and Pareek A (2003) Oryza sativa (indica cultivar-group) histidine kinase (HK1) gene, partial cds. NCBI Accession # AY211489